การปลูกผลึกโดยวิธีเอ็มโอวีพีอีและการหาลักษณะเฉพาะของสารกึ่งตัวนำ III-(III)-V-ไนไตรด์ เจือจาง: InGaPN ปลูกผลึกบน GaAs

นางสาวดาเรศ แก้วเกตุ

วิทยานิพนธ์นี้เป็นส่วนหนึ่งของการศึกษาตามหลักสูตรปริญญาวิทยาศาสตรดุษฎีบัณฑิต
สาขาวิชาฟิสิกส์ ภาควิชาฟิสิกส์
คณะวิทยาศาสตร์ จุฬาลงกรณ์มหาวิทยาลัย
ปีการศึกษา 2555

ลิขสิทธิ์ของจุฬาลงกรณ์มหาวิทยาลัย
บทคัดย่อและแฟ้มข้อมูลฉบับเต็มของวิทยานิพนธ์ตั้งแต่ปีการศึกษา 2554 ที่ให้บริการในคลังปัญญาจุฬาฯ (CUIR)
เป็นแฟ้มข้อมูลของนิสิตเจ้าของวิทยานิพนธ์ที่ส่งผ่านทางบัณฑิตวิทยาลัย
The abstract and full text of theses from the academic year 2011 in Chulalongkorn University Intellectual Repository (CUIR)
are the thesis authors' files submitted through the Graduate School.

MOVPE GROWTH AND CHARACTERIZATION OF DILUTE III-(III)-V-NITRIDE SEMICONDUCTOR: InGaPN ON GaAs

Miss Dares Kaewket

A Dissertation Submitted in Partial Fulfillment of the Requirements

for the Degree of Doctor of Philosophy Program in Physics

Department of Physics

Faculty of Science

Chulalongkorn University

Academic Year 2012

Copyright of Chulalongkorn University

Thesis Title	MOVPE GROWTH AND CHARACTERIZATION OF DILUTE III-(III)-V-NITRIDE SEMICONDUCTOR: InGaPN ON GaAs
By	Miss Dares Kaewket
Field of Study	Physics
Thesis Advisor	Assistant Professor Sakuntam Sanorpim, Ph.D.
Thesis Co-advisor	Professor Kentaro Onabe, Ph.D.
	Assistant Professor Sukkaneste Tungasmita, Ph.D.

Accepted by the Faculty of Science, Chulalongkorn University in Partial Fulfillment of the Requirements for the Doctoral Degree

.....Dean of the Faculty of Science
(Professor Supot Hannongbua, Dr. rer. nat.)

THESIS COMMITTEE

.....Chairman
(Assistant Professor Sojiphong Chatraphorn, Ph.D.)

.....Thesis Advisor
(Assistant Professor Sakuntam Sanorpim, Ph.D.)

.....Thesis Co-advisor
(Professor Kentaro Onabe, Ph.D.)

.....Thesis Co-advisor
(Assistant Professor Sukkaneste Tungasmita, Ph.D.)

.....Examiner
(Assistant Professor Somchai Kiatgamolchai, Ph.D.)

.....Examiner
(Burin Asavapibhop, Ph.D.)

.....External Examiner
(Nattaporn Chattham, Ph.D.)

ดาเรศ แก้วเกตุ : การปลูกผลึกโดยวิธีเอ็มโอวีพีอีและการหาลักษณะเฉพาะของสารกึ่งตัวนำ III-(III)-V-ไนไตรด์เจือจาง: InGaPN ปลูกผลึกบน GaAs. (MOVPE GROWTH AND CHARACTERIZATION OF DILUTE III-(III)-V-NITRIDE SEMICONDUCTOR: InGaPN ON GaAs) อ.ที่ปรึกษาวิทยานิพนธ์หลัก : ผศ.ดร.สกุลธรรม เสนาะพิมพ์, อ.ที่ปรึกษาวิทยานิพนธ์ร่วม : PROF. KENTARO ONABE, Ph.D., ผศ.ดร.สุคคเณศ ตุงคะสมิต, 85 หน้า.

วิทยานิพนธ์นี้ ลักษณะเฉพาะของ InGaPN/GaAs ที่เกี่ยวข้องกับการใช้เป็นชั้นดูดซับในเซลล์แสงอาทิตย์ถูกวิเคราะห์ เพื่อตรวจสอบการวางตัวของแถบพลังงาน บ่อศักย์ InGaPN/GaAs และ GaAs/InGaPN คุณภาพผลึกสูงถูกปลูกบนลงบนซับสเตรต GaAs (001) ด้วยวิธีเมทอลออแกนิกเวเปอร์เฟสอีพิแทกซี ผลจากโฟโตลูมิเนสเซนซ์ที่ 10K ของบ่อศักย์ แสดงพีคพิเศษในช่วงพลังงานอินฟราเรด พีคพิเศษของบ่อศักย์ GaAs/InGaPN คงอยู่ถึงอุณหภูมิ 240K ในขณะที่พีคพิเศษบ่อศักย์ InGaPN/GaAs ถูกทำให้หายไปที่อุณหภูมิประมาณ 120K สถานการณ์นี้แสดงว่าทั้งสองบ่อศักย์เป็นโครงสร้างควอนตัมชนิดที่สอง ความต่างของแถบวาเลนซ์และแถบการนำถูกประมาณเป็น 450 และ 160 meV ตามลำดับ

เพื่อที่จะศึกษาช่องว่างแถบพลังงานของ InGaPN และการเปลี่ยนแปลงของมันกับอุณหภูมิ ชั้น InGaPN ที่มีความเข้มข้นของไนโตรเจนต่าง ๆ กัน ถูกปลูกแบบสอดคล้องลงบนซับสเตรต GaAs (001) เมื่อไนโตรเจนเพิ่มขึ้น โฟโตลูมิเนสเซนซ์และโฟโตรีเฟลกแทนซ์ แสดงถึงช่องว่างแถบพลังงานที่ลดลง โฟโตลูมิเนสเซนซ์ที่ขึ้นกับอุณหภูมิพร้อมด้วยการฟิตติง แสดงให้เห็นถึงการขึ้นกับอุณหภูมิของช่องว่างแถบพลังงานของ InGaPN ที่มีผลน้อยลงอย่างมีนัยสำคัญเมื่อเพิ่มปริมาณไนโตรเจน ค่าคงที่ที่ได้จากการฟิตติงแสดงค่าที่เข้าใกล้ลักษณะเฉพาะของ III-ไนไตรด์ (คือ GaN และ InN) เมื่อเพิ่มไนโตรเจน ผลจากการกระเจิงรามานในช่วง 400 – 900 cm^{-1} แสดงลักษณะเฉพาะคล้าย GaN สิ่งนี้แสดงถึงพันธะ Ga-N มีปริมาณมากกว่าพันธะ In-N ในชิ้นงาน InGaPN ซึ่งทำให้สมบัติการขึ้นอยู่กับอุณหภูมิน้อย อาจจะเกิดจากผลของพันธะ Ga-N นี้

ภาควิชา ฟิสิกส์ ลายมือชื่อนิสิต.....

สาขาวิชา ฟิสิกส์ ลายมือชื่อ อ.ที่ปรึกษาวิทยานิพนธ์หลัก.....

ปีการศึกษา 2555 ลายมือชื่อ อ.ที่ปรึกษาวิทยานิพนธ์ร่วม.....

ลายมือชื่อ อ.ที่ปรึกษาวิทยานิพนธ์ร่วม.....

5073934623 : MAJOR PHYSICS

KEYWORDS : III-(III)-V-NITRIDE / PHOTOLUMINESCENCE / X-RAY DIFFRACTION / RAMAN SCATTERING / MOVPE

DARES KAEWKET : MOVPE GROWTH AND CHARACTERIZATION OF DILUTE III-(III)-V-NITRIDE SEMICONDUCTOR: InGaPN ON GaAs. ADVISOR : ASST. PROF. SAKUNTAM SANORPIM, Ph.D., CO-ADVISOR : PROF. KENTARO ONABE, Ph.D., ASST. PROF. SUKKANESTE TUNGASMITA, Ph.D., 85 pp.

In the dissertation, the characteristics of InGaPN/GaAs related to the using as the absorber layer in solar cell were analyzed. In order to verify the band alignment, the InGaPN/GaAs and GaAs/InGaPN quantum wells (QWs) with high structural quality were grown on (001) GaAs substrates by metalorganic vapor phase epitaxy (MOVPE). The results from 10K photoluminescence (PL) of QWs show the extra peaks in infrared energy range. The extra peak of GaAs/InGaPN QW survives for the temperature up to 240K while The extra peak of the InGaPN/GaAs QW is quenched at the temperature about 120K. This situation suggested that both QWs are the type-II quantum structures. The valence and conduction band offsets are approximated to be 450 and 160 meV, respectively.

In order to investigate the energy gap of InGaPN and its variation with temperature, the InGaPN layers with various N concentrations were coherently grown on (001) GaAs substrate. With increasing N, the results of PL and photoreflectance (PR) show that the energy gap is decreased. The temperature dependent PL together with fitting show that the temperature dependence of the bandgap energies of InGaPN layers becomes significantly weak with increasing N content. The fitting parameters show the values shift toward the III-nitride (i.e. GaN and InN) characteristic with increasing N. the Raman scattering results in the range of 400 – 900 cm^{-1} show the GaN-like characteristic. This suggests that the Ga-N bonds make a larger contribution than In-N bonds in InGaPN samples. The less dependence of bandgap on temperature property might be mostly contributed by Ga-N bonds.

Department : Physics Student's Signature .....

Field of Study : Physics Advisor's Signature .....

Academic Year : 2012 Co-advisor's Signature .....

Co-advisor's Signature .....

Acknowledgements

I would like to sincerely express my gratitude to my advisors, Assistant Professor Dr. Sakuntam Sanorpim, Professor Dr. Kentaro Onabe and Assistant Professor Dr. Sukkaneste Tungasmita for their valuable suggestion and encouragement. They gave me good experiences such as working with good guidance, participating in an international conference and English writing (journal and dissertation).

I would like to thank the Advanced Materials Physics (AMP) Research group, Professor Dr. Kentaro Onabe's laboratory, Department of Advanced Materials Science, The University of Tokyo, Japan and Professor Dr. Per Olof Holtz's laboratory, Department of Physics (IFM), Linköpings University, Sweden for their hospitality and generosity in letting me using their instruments for my research.

I am deeply indebted to Assistant Professor Dr. Sojiphong Chatraphorn, Assistant Professor Dr. Somchai Kiatgamolchai, Dr. Burin Asavapibhop and Dr. Nattaporn Chattham for taking time from their busy schedules to be on my dissertation committee. Their comments on this dissertation are also grateful appreciated.

I would like to acknowledge Thailand Research Fund through the Royal Golden Jubilee Ph.D. Program for supporting fund during my study. I wish to thank The 90^{th} Anniversary of Chulalongkorn University Fund for supporting fund for this dissertation.

I would like to acknowledge Dr. Ryuji Katayama and Dr. Shigeyuki Kuboya for their valuable discussion.

I would like to thank my colleagues; Dr. Pawinee Klangtakai, Dr. Jamreonta Parinyataramas, Papaporn Jantawongrit and many friends for useful discussion and joyful moment.

Last but not least, I would like to pay my heartfelt thanks to my family for love, understanding, and supports during my study.

CONTENTS

Chapter **page**

List of Tables

Table **page**

List of Figures

CHAPTER I

Introduction

1.1 Overview and motivation

Dilute III-(III)-V-nitride semiconductors are very interesting material due to their unique physical properties. This type of III-V alloy contains a small amount of nitrogen (N). It is well known that an incorporation of a few percents of N leads to a large reduction of bandgap. For example, the addition of 1% of N into GaAs reduced the bandgap from 1.42 to 1.25 eV at room temperature [1]. Moreover, for the quaternary alloys such as InGaPN and InGaAsN, the lattice constant can be adjusted by controlling the compositions of N and indium (In). Since, an In atom has a larger atomic size compared to that of gallium (Ga), phosphorus (P), arsenic (As) and N atoms, so an addition of In results in an increasing of the lattice constant of the alloy. On the other hand, adding N results in a decreasing of the lattice constant. So, the lattice match condition can be reached with many commercially available substrates such as GaAs [2 - 6] or Ge [7, 8]. Since both its bandgap and lattice constant can be adjusted by controlling the alloy compositions, this material is expected to be “engineered semiconductor”. Their potential applications conclude of optoelectronic and electronic devices such as light emitting diodes (LEDs), laser diodes (LDs), heterojunction bipolar transistors and solar cells.

Nowadays, the solar cells with III-V semiconductors as an absorber layers are of being interested due to very high conversion efficiency. Figure 1.1 is the plot of record solar cell efficiencies for different technologies. As seen from the figure, the III-V multijunction solar cells have the highest conversion efficiency. This type of solar cell is generally used as a power source for space stations or satellites in space due to its high efficiency and light weight. At the present (year 2011), the highest

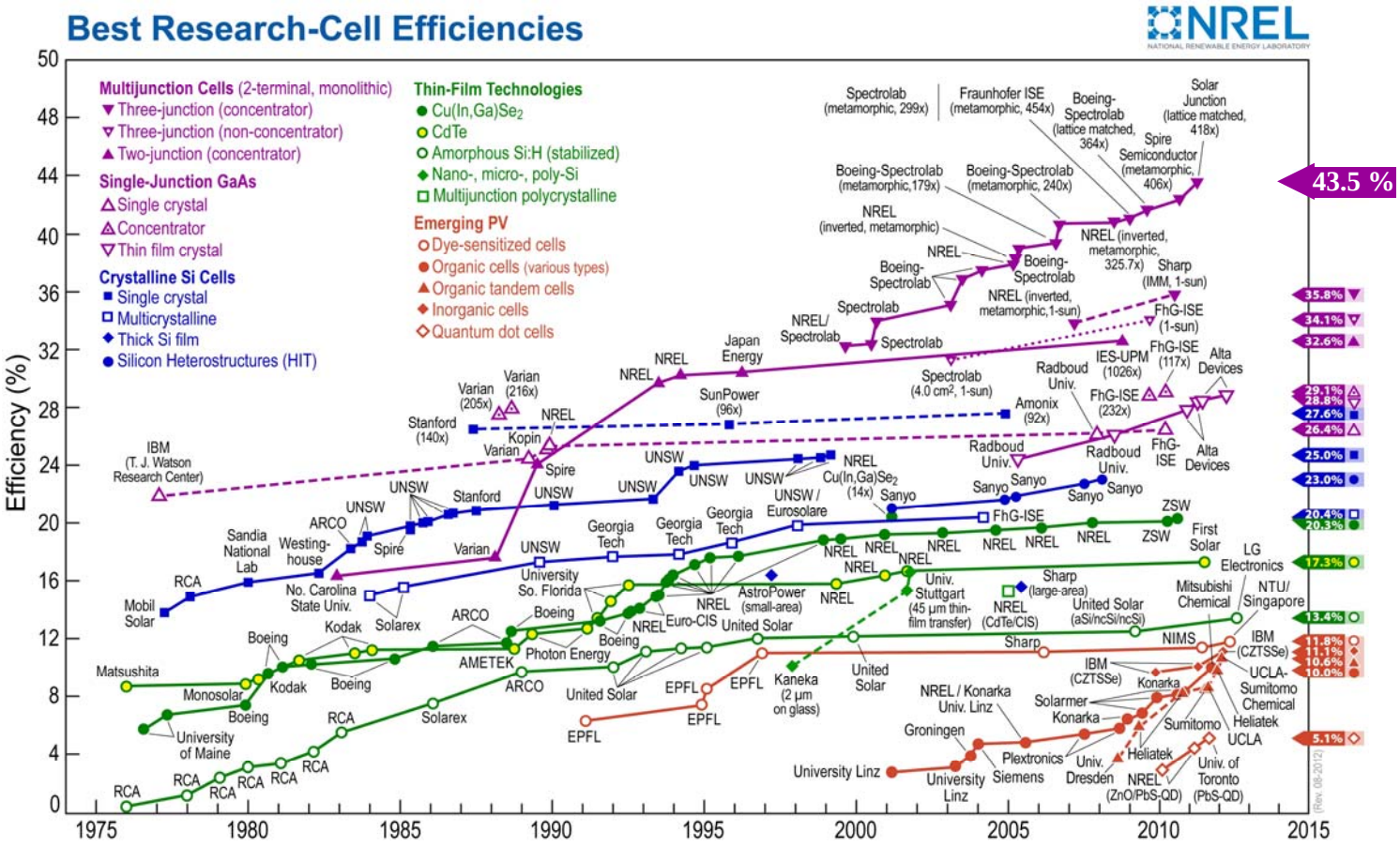

Figure 1.1: Plot of record solar cell efficiencies for different technologies, showing the high efficiency for III-V multijunction solar cells (http://www.nrel.gov).

efficiency was recorded at 43.5% for concentrator multijunction solar cell with dilute nitride absorber (InGaP/GaAs/InGaAsN) [9]. This high efficiency of concentrator III-V multijunction solar cells proposes a lowering electricity production and installation costs [10]. This leads III-V multijunction solar cells are used as terrestrial photovoltaic devices not only in the space [11]. The important keys to approach the maximum efficiency are the variety of semiconductors with different bandgaps and lattice-match conditions. This is a challenge for the use of quaternary dilute III-III-V-nitride semiconductors such as InGaAsN and InGaPN as the absorber layer in multijunction solar cells.

Especially, InGaPN, energy gap of this material can possibly be varied between 1.9 eV (bandgap of InGaP) and 0.8 eV (bandgap of InN), while the lattice constant can be still lattice-matched to GaAs. Figure 1.2 shows the bandgap energy versus the lattice constant for III-V semiconductors [12], including InGaPN. In

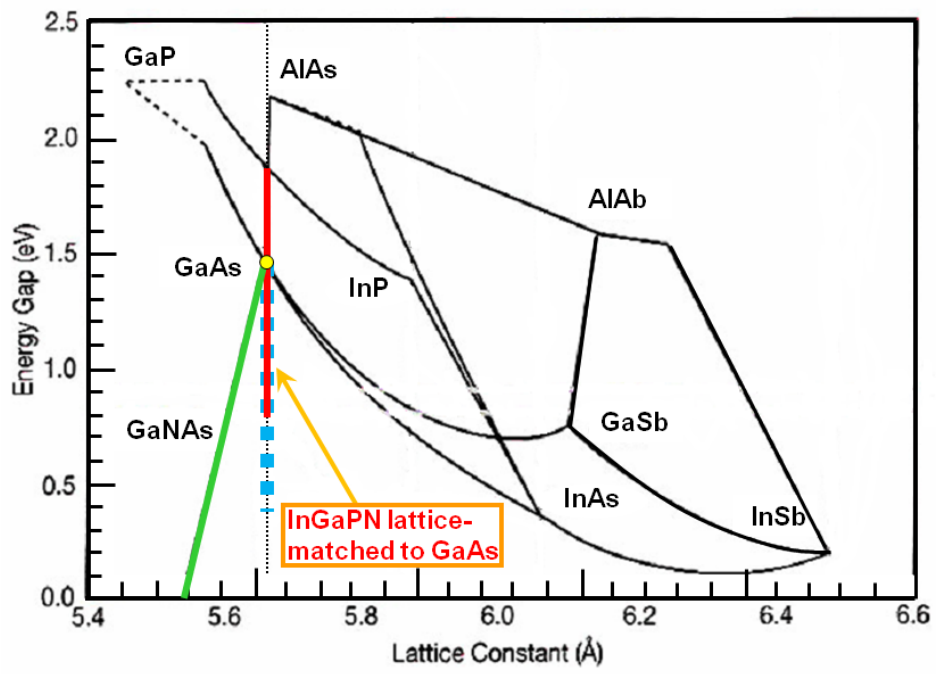

Figure 1.2: The relationship between bandgap and lattice constants of III-V semiconductors [12]. The red solid line indicates the bandgap of InGaPN, while the blue dashed line indicates the bandgap of InGaAsN. The green solid line indicates the bandgap of GaAsN showing an effect of the N incorporation.

practical, the interesting energy gap of InGaPN is not lower than 1.42 eV which is the GaAs energy gap, because InGaAsN better provide the energy gap in this region. The energy gap around 1.9 – 1.42 eV of InGaPN is suitable for using as the upper absorber layer of multijunction solar cell [13]. The adjustable both bandgap and lattice constant of InGaPN make this material is more advantage over than InGaP which has energy gap around 1.8 - 1.9 eV for lattice-matching to GaAs [14, 15]. These adjustable properties of InGaPN potentially open promising prospects for design and fabrication of higher efficiency III-V multijunction solar cells in the future.

Currently, the material quality of dilute III-(III)-V-nitride layers still not reaches high quality level. This might cause the degradation of electrical property in solar cells [3, 16, 17]. So, it is a challenge of crystal growth technology to grow the nitrogen containing InGaPN layers with a high optical and crystal quality. Recently, the III-V solar cell mass production relies on metal organic vapor phase epitaxy (MOVPE) process [18, 19]. So, the information obtained from researching with MOVPE grown samples can support the large scale production.

1.2 Objectives and scope of the dissertation

From the above motivation, it is very interesting to study InGaPN semiconductor in point of view of the possibility for the absorber layer application.

For solar cell application, the separation of electrons and holes is important. In this case, the type-II band lineup between two absorbers is advantageous. In this dissertation, InGaPN/GaAs quantum well (QW) and GaAs/InGaPN QW have been grown by MOVPE for investigating the band lineup between InGaPN and GaAs. In addition, the InGaPN/GaAs bulk layers with various N concentrations have been grown in order to investigate the effect of N incorporation on the structural and electronic properties.

In order to verify the above materials properties, high resolution X-ray diffraction (HRXRD) has been used as a tool to determine the composition and crystal quality. Bandgap of InGaPN has been investigated by the temperature dependent photoluminescence (PL) and photoreflectance (PR). The Raman scattering

measurement has been performed to confirm the incorporation of N, which is indicated by the In-N or Ga-N related bonds.

It is believed that the information obtained from this dissertation can fulfills the databases for fabrication of the InGaPN based high-efficiency III-V solar cells.

1.3 Organization of the dissertation

The dissertation is organized as follows:

In chapter I, as described above, the overview of dilute III-(III)-V-nitride semiconductors are introduced, including the motivation. Especially InGaPN is focused.

In chapter II, the solar cell is introduced. In addition, the literature and in-depth physical properties of dilute III-(III)-V-nitride semiconductors are described.

In chapter III, the growth and characterization methods, including the experiment are presented.

In chapter IV, the results are divided into 4 papers. The connection of papers is initially presented.

Finally, conclusion and suggestion of the dissertation are given in chapter V.

CHAPTER II

Third generation solar cell and dilute-III-(III)-V-nitride prospect

2.1 Third generation solar cell

It is known that the efficiency of a solar cell consisting of a single absorber layer is theoretically limited to be about 40.8% for the absorber with optimal bandgap with E_g = 1.1 eV [13]. It is due to i) the thermalization loss, ii) non-absorption loss (or transmission loss), iii) recombination loss, iv) junction loss and v) contact loss [13, 20]. The major losses come from the thermalization of hot carriers and the non-absorption loss which account for approximately 50% of incident solar energy [21, 22]. This situation is found in the first and second generation solar cells that rely on a homojunction silicon-base wafer and thin film technology, respectively.

For reaching higher efficiency, the major losses need to be reduced. This leads to the concepts of the third generation solar cells that allow utilization of sunlight than the typical homojunction solar cells. The most well-known of third generation solar cells is the multijunction solar cell.

2.1.1 Multijunction solar cell

One way to extend the solar spectrum utilization is subdividing the solar spectrum into the small energy ranges. These several solar parts are then absorbed by the semiconductors, which have the suitable bandgap. One approach is stacking cells above each other, using multi-absorber layers. The high-bandgap top cell converts the shortest wavelength fraction and permits the longer wavelength to convert at lower cells, which include lower bandgap semiconductors, in the stack. A schematic

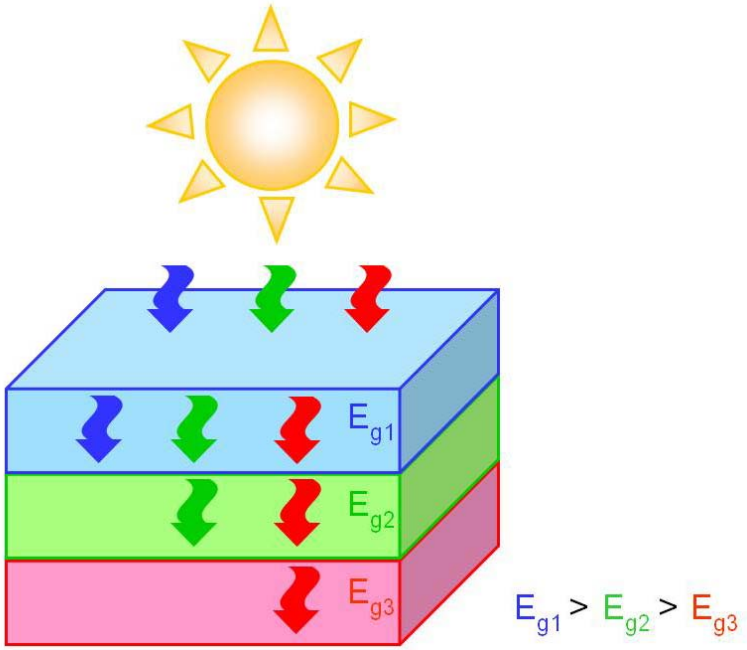

Figure 2.1: Schematic drawing shows the light absorption of multijunction solar cell.

diagram is shown in Fig. 2.1. Because the cells are connected via p-n junction, this system is called multijunction solar cell. For this system, it is expected that the more number of p-n junctions, the less thermalization and transmission losses [23], resulting in higher efficiency.

In practical, each absorber of the multijunction solar cell connects with each other by the series connection. It has long been known that the efficiency is limited by the absorber that provides the minimum current. Hence, the equal currents from every absorber are desired. The optimal energy gaps of absorbers are calculated in relation to the solar spectrum. Table 2.1 shows the optimal bandgaps for a range of multijunction cell designs and their limiting efficiencies [13]. However, in practical, it is difficult to follow the optimization due to limiting of available materials with desired bandgaps. Figure 2.2 shows the commercial three-junction structure with InGaP/InGaAs/Ge absorbers and expected four-junction structure with InGaP/InGaAs/InGaAsN/Ge absorbers for higher efficiency [23].

No. of cells	Optimal bandgaps (eV)						Efficiencies %
	E1	E2	E3	E4	E5	E6	
1	1.11						40.8
2	0.77	1.55					55.5
3	0.61	1.15	1.82				63.2
4	0.51	0.94	1.39	2.02			67.9
5	0.44	0.81	1.16	1.58	2.18		71.1
6	0.38	0.71	1.01	1.33	1.72	2.31	73.4
∞							86.8

Table 2.1: Limiting efficiencies and optimal bandgaps for a range of multijunction cells [13] (in case of direct sunlight and series connected)

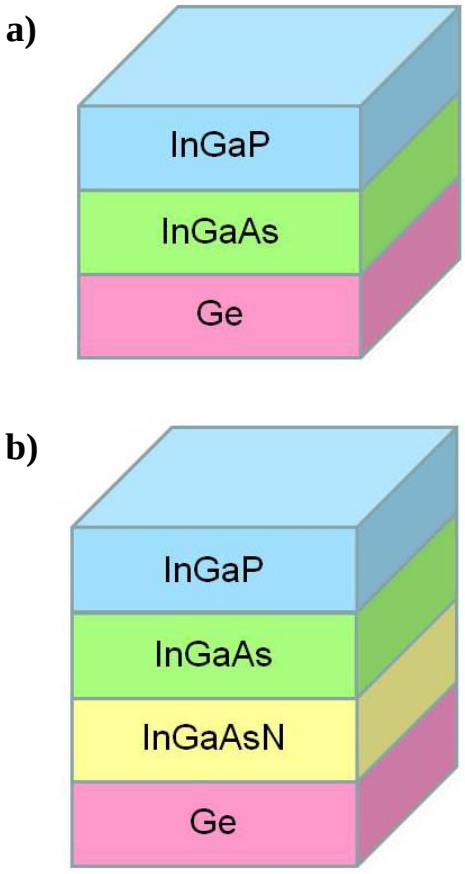

Figure 2.2: a) The commercial structure with InGaP/InGaAs/Ge absorbers and b) expected structure with InGaP/InGaAs/InGaAsN/Ge absorbers for higher efficiency.

2.2 Dilute-III-(III)-V-nitride : InGaPN

InGaPN is a novel quaternary material in the group of dilute III-V-nitride semiconductors that can be lattice-matched to the conventional substrates such as GaAs [24] and GaP [25]. Its potential applications conclude of optoelectronic and electronic devices such as light emitting diodes (LEDs), laser diodes (LDs) [26, 27], heterojunction bipolar transistors and solar cells [24]. It is known that an incorporation of a few percent of N into InGaP [28, 29] drastically reduces the bandgap due to huge bandgap bowing, which is commonly found in the III-V-N semiconductors, such as GaAsN [30], GaPN [31] and InGaAsN [32]. As a result, InGaPN is expected to be "engineered semiconductor", since both its bandgap and lattice parameters can be adjusted by controlling the incorporation of In and N.

Dilute-III-V-nitride semiconductors are in the type of highly mismatched alloys which have large bandgap reduction with small N incorporation. One model that can describe this situation is the band anticrossing (BAC) model [33, 34]. This model describes as follow; for dilute III-V-nitride semiconductors, the substituted nitrogen atoms form the highly localized state that generally locates very close to the host conduction band state. From a point of view of quantum mechanics, the interaction between two states makes two effective sub-bands, E_+ and E_- which described by the equation

$$E_{\pm} = \frac{1}{2}\left\{ \left(E_{\mathrm{N}} + E_{\Gamma}\right) \pm \sqrt{\left(E_{\mathrm{N}} - E_{\Gamma}\right)^2 + 4V^2 y} \right\} \qquad (2.1)$$

where E_{Γ} is the energy of unperturbed conduction band state, E_{N} is the energy of localized state. Both energies are relative to the top of the valence band. V is the interaction potential between the two bands and y is the N concentration. Figure 2.3 illustrates the effect of band anticrossing on the Γ band structure in case: a) the localized state resonant with the conduction band and b) the localized state locates below the conduction band [35]. This BAC model gives good agreement with the experimental results of GaAsN as shown in Fig. 2.4 [35]. For InGaPN, there are only few reports about band structure for this material. The BAC model is also used to describe the band structure of InGaPN. The value of E_{N} = 2.0 – 2.1 eV and V = 1.4 -1.7 eV [36 - 38] are reported for InGaPN grown by molecular beam epitaxy (MBE).

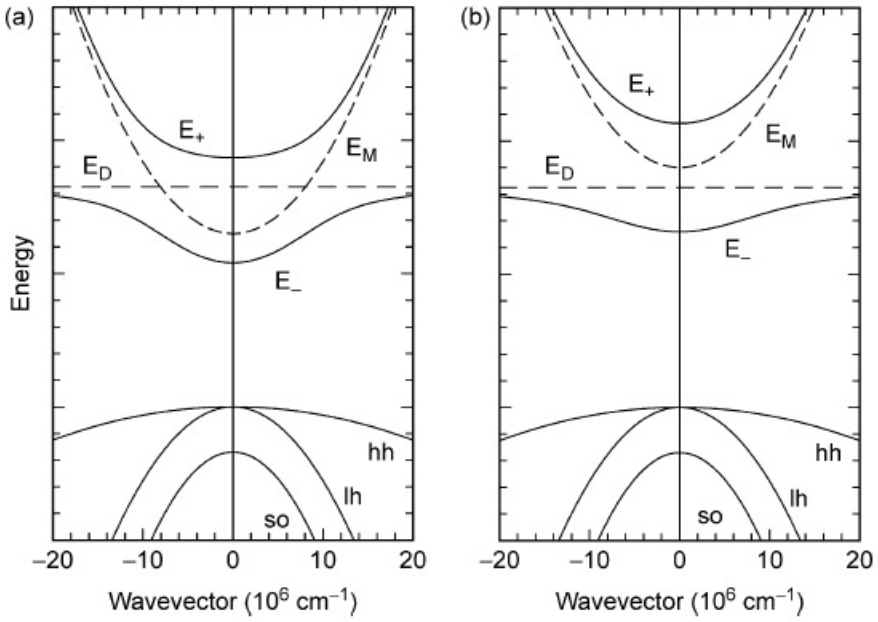

Figure 2.3: Illustration of the effect of band anticrossing on the Γ band structure in case: a) the localized state resonant with the conduction band and b) the localized state locates below the conduction band [35].

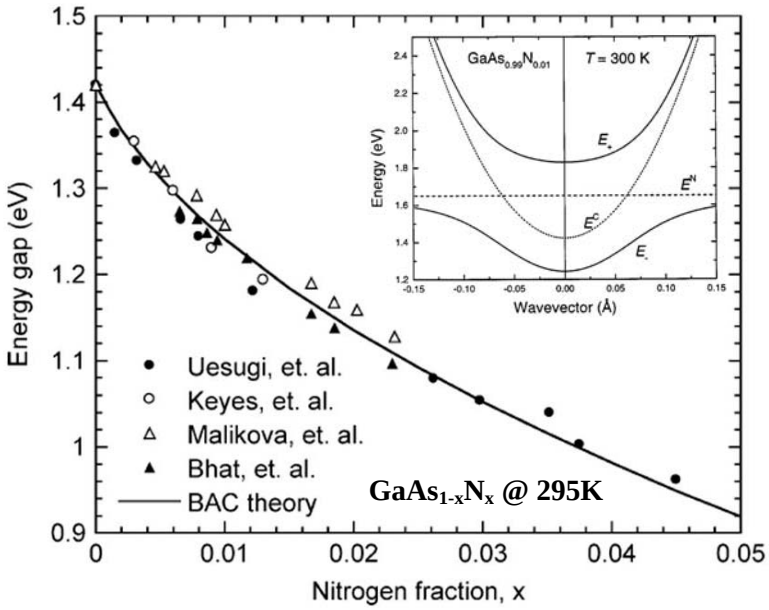

Figure 2.4: The comparison between the experimental data observed by several research groups and the calculation based on BAC model [35]. The inset shows the calculation of $GaAs_{0.99}N_{0.01}$ from BAC model.

InGaPN can provide the bandgap 0.8 - 1.9 eV with lattice matching to GaAs (see Fig 1.2). The lattice match condition is the important for multijunction solar cell fabrication. Unlike the light emitting devices that the lattice mismatch structure is allow because the thickness of active layer are normally less than the critical thickness, the thickness of the solar cell absorber layer is on the order of micron. So, the lattice match structure is important for prevention of structural defect that cause the degradation of solar cell [39]. There is report that the lattice mismatch as small as 0.01% significantly reduces the current created by the solar cell [40]. Hence, InGaPN is potentially use as the top or under top layer of solar cell. The wide range tunable bandgap of InGaPN provide the fabrication of structures with more junctions possibly. Recently (year 2011), the multijunction solar cell gives the latest efficiency at 43.5% (1000 sun) with dilute nitride absorber (InGaP/GaAs/InGaAsN) [9].

According to the BAC model, dilute III-V-nitride semiconductors are the highly mismatched alloys which have the intermediate band (E_-) in the forbidden gap. Hence, they have opportunity to produce as multiband solar cell. The multiband solar cell is one type of third generation solar cells. For this type, the semiconductor that have the impurity level or intermediate band line in the forbidden gap is using. The impurity or intermediate states provide the stepping-stone for low energy photons to excite the carriers across the gap via two-step process [41, 42]. The dilute III-V-nitride multiband solar cell is first reported by N. López et al. [43], which is $GaAs_{1-x}N_x$. Their results show that the $GaAs_{1-x}N_x$ photovoltaic device with blocking layer can absorb the photon energy 1.1 – 3.2 eV. However, the minority life time is short which has been found in InGaAsN [44]. Nevertheless, recently there is the way to improve the electrical properties of dilute III-V-nitride absorbers which can be seen from the achievement of the multijunction solar cell fabrication with dilute nitride absorber. The intermediate band that also observed in InGaPN leads this material to be the potential use as the multiband solar cell.

Moreover, due to the dilute III-V nitride semiconductors exhibit the strong localization, they suitable for third generation solar cells which focus on the improving efficiency by using the semiconductor which have states in forbidden gap. Those concepts of new generation solar cells provide high efficiency with using materials economically which result in lower cost.

InGaPN has the range of bandgap that not too high for collecting the solar spectrum and not too low for preventing the thermalization loss. The adjustable bandgap of InGaPN is useful for optimizing the solar utilization of new generation solar cells.

CHAPTER III

Experimental methods

3.1 Metalorganic vapor phase epitaxy

Metaloganic vapor phase epitaxy (MOVPE) growth method is done by flowing metalorganic gases into the reactor chamber which has the substrate. The precursors of metals (in these case, III-column elements) are the metalorganic compounds, which have the metal element bonds to the organic group such as methyl (CH_3), ethyl (C_2H_5) and butyl (C_4H_9). Nowadays, the organic precursors for V-column elements are also available. These organic precursors have low decomposition temperature, relatively high vapor pressure [45]. This suitable for growth of dilute nitride materials, which need low growth temperature, due to it is non-equilibrium process [46]. In addition, these organic compounds are less toxic than hydride sources such as AsH_3 and PH_3.

In this work, we used trimethylindium (TMIn), trimethylgallium (TMGa), tertiarybutylphosphine (TBP), tertiarybutylarsine (TBAs) and dimethylhydrazine (DMHy), as the precursors of In, Ga, P, As and N, respectively.

Most of the organic compounds are liquid phase at room temperature, such as TMGa, TBP, TBAs and DMHy (in the case of TMIn, it is the solid). Hence, they require the bubbling process that converts the liquid or solid phase to vapor phase. In the process, the inert carrier gas such as H_2 is flowed into the bubbler. This H_2 gas dissolves and carries the precursor then flows out from the bubbler. The bubbler is placed in the bath for controlling the temperature of vapor.

Vapor partial pressure of metalorganic (MO) precursors can be expressed as;

$$P_{\mathrm{MO}} = 10^{a-(b/T)} \ \text{Torr} \qquad (3.1)$$

where *a* and *b* are the constants provided by the manufacturer. *T* is the temperature controlled by the bath.

Molar flow rate of the MO precursor can be given by;

$$F_{\mathrm{N,\,MO}} = \frac{1}{22400} \times \frac{P_{\mathrm{MO}}}{P_{\mathrm{total}}} \times F_{\mathrm{V,\,total}} \tag{3.2}$$

where $F_{\mathrm{N,\,MO}}$ is the molar flow rate of the MO precursor (mol/min), P_{MO} is the partial vapor pressure of the MO precursor (Torr) while P_{total} is the total pressure of gas mixtures (the summation of the partial pressure of the MO precursor and the partial pressure of the carrier gas, in this case P_{total} = 760 Torr). $F_{\mathrm{V,\,total}}$ is the total volume flow rate of gas mixtures (sccm). In general, the volume flow rate of carrier gas is much larger than the MO gas, so $F_{\mathrm{V,\,total}}$ is approximated to be the volume flow rate of the carrier gas.

Schematic of MOVPE system used in Onabe Laboratory, The University of Tokyo is simply shown in Fig. 3.1. The mixture of metalorganic and H_2 gases are flowed into the horizontal cold-wall reactor chamber which made from quartz. The graphite susceptor is preferentially heated by radio frequency (RF) coil.

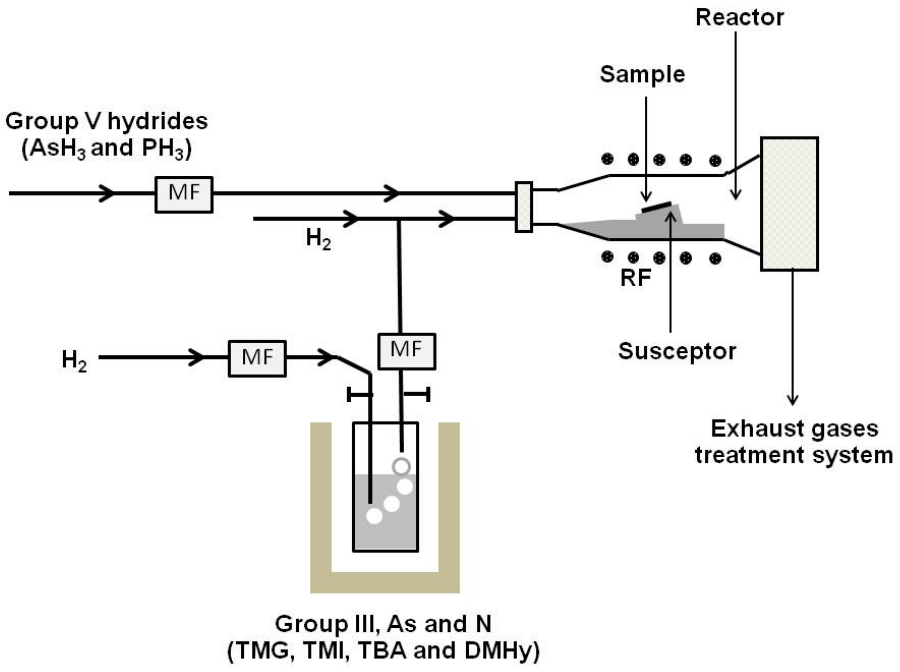

Figure 3.1: Schematic of MOVPE system

3.1.1 Growth of samples

The samples studied in this work were grown at Onabe Laboratory, The University of Tokyo, Japan. In this work, GaAs (001) wafer was used as the substrate. The $In_{0.528}Ga_{0.472}P_{1-y}N_y$ bulk layers as well as the $In_{0.528}Ga_{0.472}P_{0.973}N_{0.027}$/GaAs and GaAs/$In_{0.528}Ga_{0.472}P_{0.973}N_{0.027}$ single quantum wells (QW) were grown. A GaAs buffer and the $In_{0.528}Ga_{0.472}P_{1-y}N_y$ layers were grown at 650 °C and 520°C, respectively. Growth pressure was kept at 60 Torr. [TMI]/III ratio was maintained at 0.63. For the $In_{0.528}Ga_{0.472}P_{1-y}N_y$ bulk layers, in order to change the N concentration, the [DMHy] flow rates were varied as 0, 600, 1000 and 1500 µmol/min. For the QW samples, the the [DMHy] flow rates for the growth of $In_{0.528}Ga_{0.472}P_{0.973}N_{0.027}$ layer was 1500 µmol/min. The thickness of well and cap layers are around 7 nm and 28 nm, respectively. The GaAs buffer of $In_{0.528}Ga_{0.472}P_{0.973}N_{0.027}$/GaAs QW acts as the bottom barrier.

The sample structures are shown in Fig. 3.2.

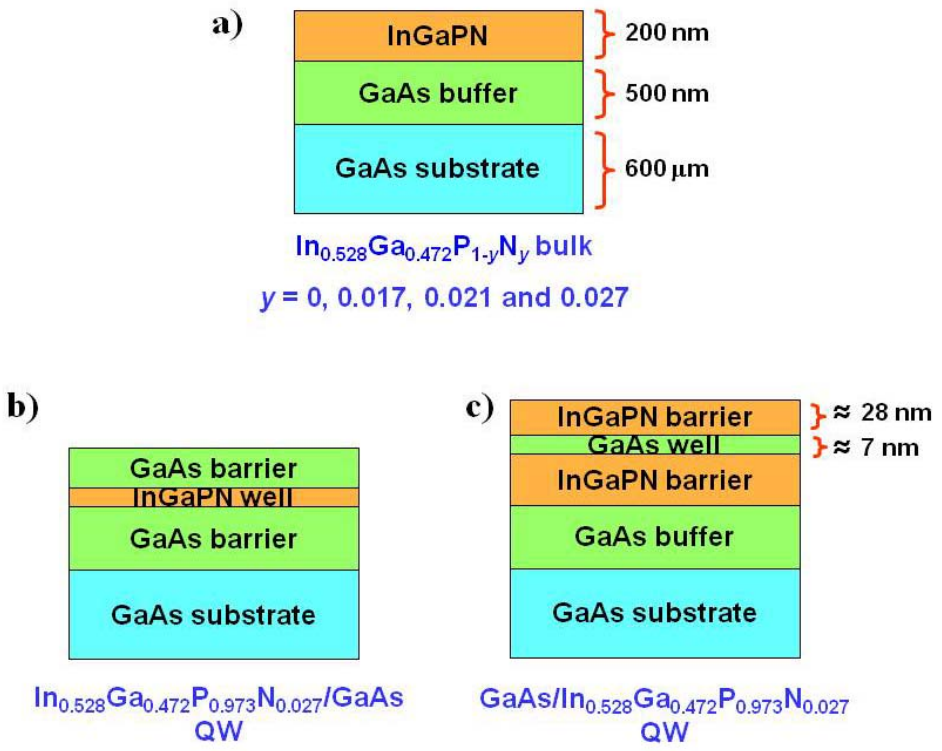

Figure 3.2: Sample structures; a) $In_{0.528}Ga_{0.472}P_{1-y}N_y$ bulk structure, b) $In_{0.528}Ga_{0.472}P_{0.973}N_{0.027}$/GaAs QW and c) GaAs/ $In_{0.528}Ga_{0.472}P_{0.973}N_{0.027}$ QW

3.2 High resolution X-ray diffraction

High resolution X-ray diffraction (HRXRD) is the versatile technique that uses the X-ray beam to probe the lattice parameters and structural properties. The X-ray beam is projected onto the sample and then is diffracted by the atomic planes in the sample. The d-spacing between the atomic planes cause the path difference of the diffracted X-ray beam and results in the diffraction patterns. The obtained diffraction patterns concern the composition, the uniformity of each layer, their thickness, the built-in strain and strain relaxation, the lattice parameters and the lattice mismatch. There are possible five structures related to strain that occur for epitaxial film; a) lattice-matched, b) fully compressive strain, c) fully tensile strain d) partially relaxed and e) fully relaxed. The HRXRD results can determine those strain properties.

The HRXRD measurement was done using the Philips X'Pert at The University of Tokyo, Japan. The HRXRD setup is shown in Fig. 3.3. The X-ray beam is emitted from the X-ray tube. In general, the X-ray beam from the anode contains three sub-wavelengths i.e. $K_{\alpha 1}$, $K_{\alpha 2}$ and K_{β}. The $K_{\alpha 1}$ radiation at a wavelength of 1.54056 Å is selected for the experiment. The other components are eliminated by the monochromator. This monochromator consists of an X-ray mirror and four (220) Germanium crystals which eliminate the K_{β} and $K_{\alpha 2}$ radiations, respectively. The

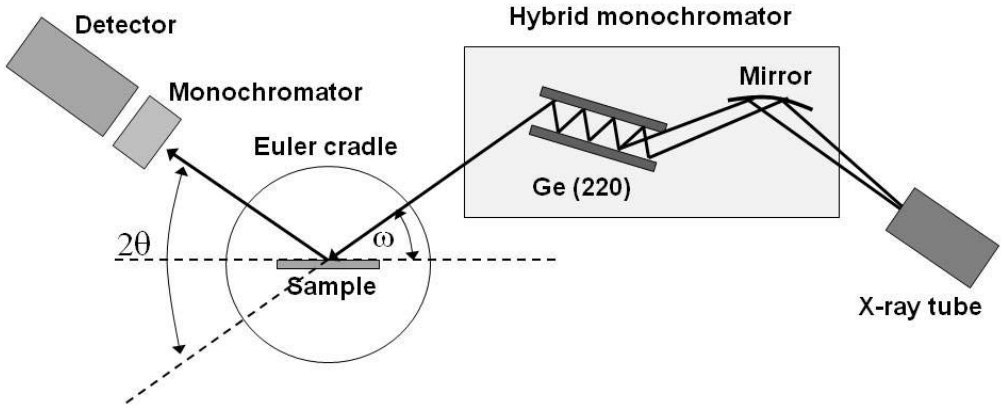

Figure 3.3: Schematic of the HRXRD system

sample is placed on the *x*-*y*-*z* stage within an Euler cradle. This Euler cradle can be moved in the direction of the incident angle (ω), the angle around the surface normal (φ) and the angle around an in-plane horizontal direction (ψ). The X-ray diffracted beam from the sample passes through the analyzer which contains the (220) Germanium crystals. This analyzer acts as the slit that constrains the detector to receive the diffracted beam in the narrow angle. Finally, the intensity of the X-ray diffracted beam is counted by the detector.

There are four important modes done by HRXRD

a) ω-scan

In this mode, the value of 2θ is fixed while the ω is varied. The orientation of the intentional Bragg planes (ex. (004) plane) is observed. In the other word, the tilted mosaic structure is probed. Practically, the Bragg angle is fixed (the positions of the x-ray tube and detector are fixed) while the sample is rocked. The range of ω-scan is about 2 degrees. A graph of the intensity versus the ω angle is plotted. This graph is often called "rocking curve".

b) 2θ-scan

This mode is done by varying the value of 2θ. The result shows the d-spacing fluctuation of one Bragg plane that we intentionally observe. In this mode, the angle of the detector is varied while the position of the X-ray tube and the sample is fixed.

c) 2θ/ω-scan

In this mode, the Bragg angle is varied. The d-spacing of each layer can be distinguished. The different d-spacing is due to the different lattice parameters. Practically, the X-ray tube is fixed. The 2θ and ω angle are varied by moving the detector and sample, respectively.

d) 2θ/ω-ω map and reciprocal space map

In this mode, the Bragg angle is varied (2θ/ω-scan). Moreover, the ω-scan is also done for each Bragg angle. Typically, the *x*-axis is 2θ range while the *y*-axis is ω range. The *z*-axis is the related intensity. Hence, this 3-axes graph contains the information about the lattice parameters, mosaic structure and strain of every layer in the sample. This 2θ/ω-ω map can be converted to the reciprocal space (*hkl*) map and vice versa. The *h* and *k* are directly related to the in-plane lattice constant ($a_{//}$) while *l*

is related to the out of plane lattice constant ($a_{\perp}$). It is easy to observe the strain property from the reciprocal space map.

The combination HRXRD results from both symmetric plane (ex. (004)) and asymmetric plane (ex. (115)) provide the complete information of lattice parameters of the sample and hence the related composition.

3.3 Photoluminescence

Photoluminescence (PL) is a versatile and contactless technique to probe the electronic structure in semiconductor. The intermediate states in forbidden gap can be possibly observed. This technique is simply performed by projecting monochromatic light (photon) that has appropriate energy (typically higher than the value of the probed energy gap) onto the sample. The photon is absorbed by the sample and then the electron in the valence band is excited to the conduction band, leaves the hole in the valence band. The electron-hole pair is created. The excited electron is unstable so it relaxes down to the conduction band minima and then recombines to the hole in the valence band by releasing the excess energy. This released energy can be in a form of light (or photon) that called the luminescence. Because the exciting source is light or photon hence this technique is called the photoluminescence (PL). The schematic PL set up is shown in Fig. 3.4. Because the photons are emitted in the direction of

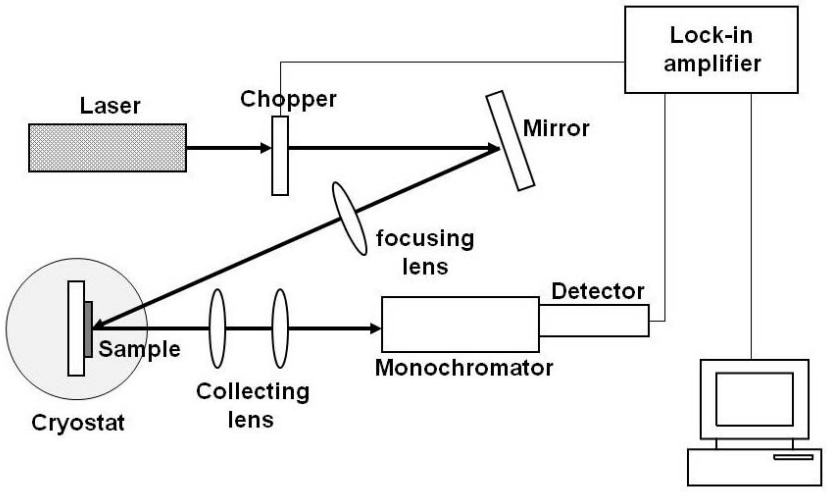

Figure 3.4: Schematic of PL set up

perpendicular to the sample's surface, so the detector is placed in front of the sample. In general, in order to gain initial information, PL is performed at low temperature in order to avoid the effect of thermalization and lattice vibration (phonon) interaction that causes low PL intensity and broad PL line shape, respectively.

The PL measurement was performed at Onabe Lab, University of Tokyo. The 488 nm-line of argon ion laser was employed as an excitation source. The luminescence signal was dispersed by a 0.3 m single monochromator and detected by an InGaAs detector (in infrared wavelength region) and a Si-photodetector (in visible wavelength region). A standard lock-in technique is used. The samples were cooled by helium closed system cryostat.

3.3.1 Temperature dependent PL

The temperature dependent PL can provides information about the variation of bandgap with temperature, the transition of carriers related to the temperature and localize states which line in the forbidden gap. Moreover, fitting data with the related equations, the value of the energy gap related to temperature and involved parameters are obtained.

The decreasing of energy gap with increasing temperature is believed to arise from two mechanisms that are the thermal expansion of the lattice and the electron-phonon interaction [47]. The later is the major contribution which is described by

$$T << \theta, \quad E_g(T) \propto T^2 \tag{3.3}$$

$$T >> \theta, \quad E_g(T) \propto T \tag{3.4}$$

where $E_g(T)$ is the energy gap at temperature T and θ is the Debye temperature. In 1967, Y. P. Varshni proposed the empirical relation that is described by the equation [47];

$$E_g(T) = E_g(0) - \frac{\alpha T^2}{\beta + T} \tag{3.5}$$

where $E_g(T)$ is the energy gap at temperature T, $E_g(0)$ is the energy gap at 0K, α and β are the fitting constants. Another model bases on the concept that the energy gap decreases proportional to Bose-Einstein statistic of phonon absorption and emission. This concept has been first proposed by L. Viña *et al* [48]. In 1997, R. Pässler

has developed the model [49] that can be simplified to the Bose-Einstein model. The expression of the single-oscillator model [50] is

$$E_g(T) = E_g(0) - \frac{\gamma\Theta}{\exp(\Theta/T) - 1} \tag{3.6}$$

where γ and Θ are the fitting constants. γ is the limiting magnitude of the slope of the $E_g(T)$ curve in high-temperature (asymptote line) and Θ is the average phonon temperature. The value of $\Theta/2$ is the point on the temperature scale where high-temperature asymptote meets the straight line of $E_g(0)$ (see Fig. 3.5). By expanding the single-oscillator equation with Taylor series in case of $T>>\Theta$, these equation can be reduced to Varshni expression with $\gamma = \alpha$ and $\Theta = 2\beta$.

3.3.2 Luminescence from QW

The luminescence from quantum well structure is classified into two situations according to band alignments. First is type-I QW, in this structure, the electron recombines to the hole in the same layer. The related emission has the energy larger than the energy gap of the well layer due to the quantum confinement energy levels of

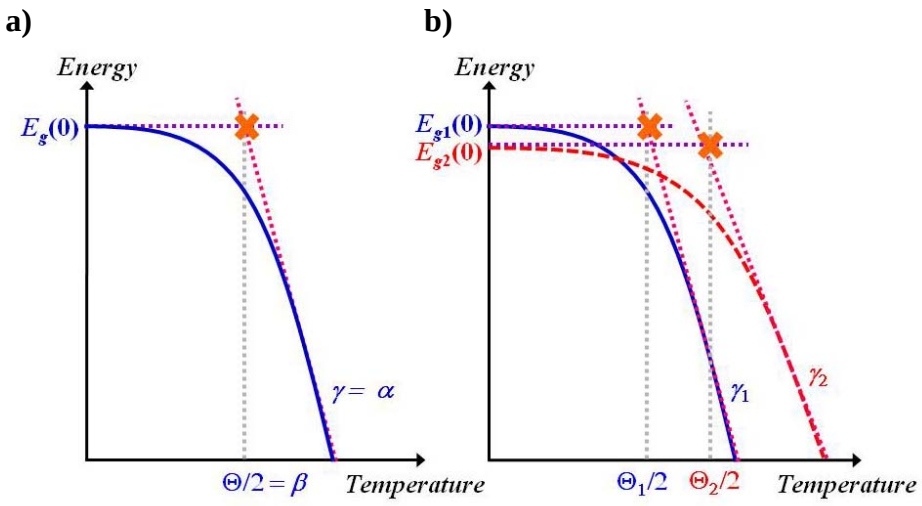

Figure 3.5: a) relation of fitted parameters obtained from Varshni and single-oscillator models, b) the comparison of bandgap variation of two materials (subscripted by 1 and 2), in this case $\Theta_1 < \Theta_2$ and $\gamma_1 > \gamma_2$

both electron and hole. Another type is type-II QW, in this structure, the electron recombines to the hole in different layer. The emissions related to the band alignments are depicted in Fig. 3.6. The difference of the conduction band edges of well and barrier layers is called "the conduction band offset, ΔE_C" and that of valence band edges is called "the valence band offset, ΔE_V".

3.3.3 Luminescence of dilute-III-V-nitride semiconductors

Typically, the temperature dependent PL results of dilute-III-V-nitride semiconductors which plotted the temperatures versus peak energies often shows the invert s-shape characteristic [51]. This phenomenon can be explained by the transition of excitons via localize states. The exciton is a one type of carriers in semiconductors. Because the free electron and hole have the opposite charges, they are attracted to

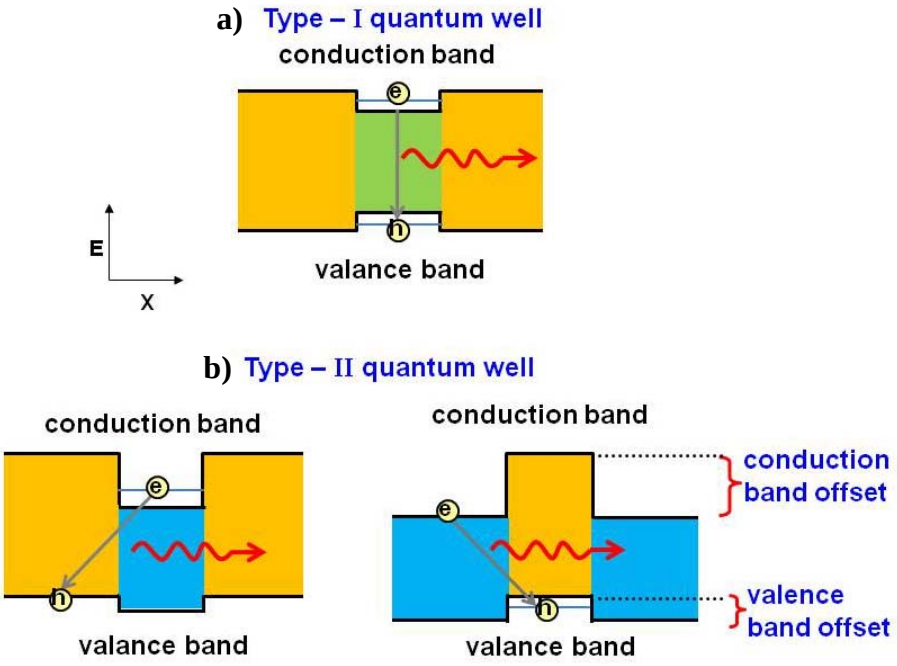

Figure 3.6: a) the luminescence from type-I QW and b) the luminescence from type-II QW

each other by the Coulomb's force. The electron orbits around the hole like the hydrogen atom and exhibits as the neutral carriers. The localize states observed in dilute-III-V-nitride alloys are described by the fluctuation in the sample. The fluctuation causes the rough conduction and valence band edges which shown in Fig.3.7. The temperature dependent PL results of $In_{0.528}Ga_{0.472}P_{0.979}N_{0.021}$/GaAs bulk is illustrated in Fig. 3.8 for an example. At 10K the excitons are trapped in the

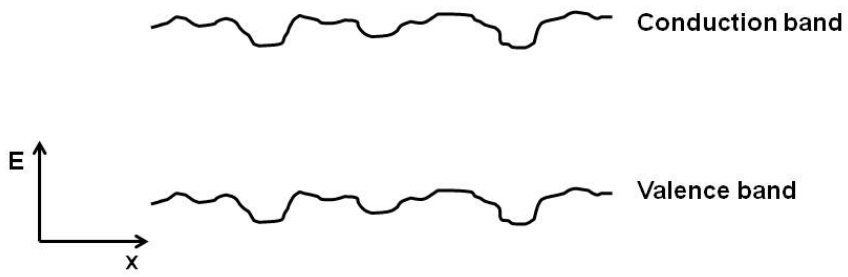

Figure 3.7: The rough band edges which activated by alloy fluctuation

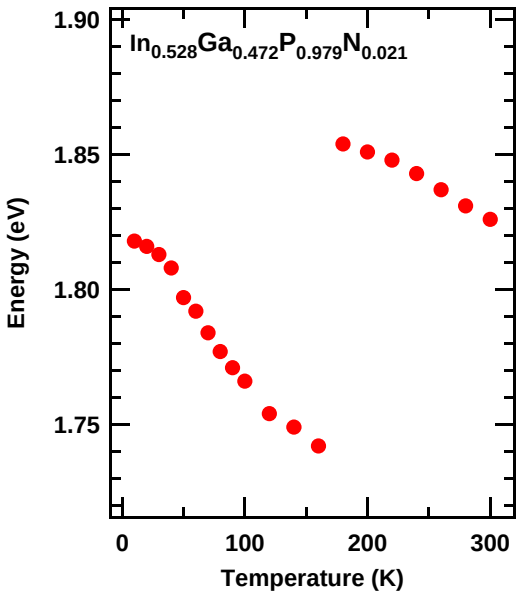

Figure 3.8: The temperature dependent PL results of $In_{0.528}Ga_{0.472}P_{0.979}N_{0.021}$/GaAs bulk

localize state. With increasing temperature (<160K), the excitons gain enough thermal energy to escape from old localize state but re-trapped by other localize state with lower energy. At the temperature higher than 160K, the excitons receive enough thermal energy to escape from most of localize states and can reach to alloy conduction band edge. Hence, in the temperature range of 180 – 300K, the PL peak energy exhibits red-shift with increasing temperature due to the decreasing of bandgap.

3.4 Photoreflectance

In photoreflectance (PR) technique, the modulating light source is projected to the sample. This light beam (typically, have the energy higher than the bandgap of the examined sample) creates the electron-hole pairs that change the reflectivity of the sample. Another light source is used to probe the modulated reflectivity of the sample. The normalized change of the reflectivity coefficient is defined as

$$\frac{\Delta R}{R} = \frac{R - R'}{R} \tag{3.7}$$

where R and R' are the reflectivity coefficients when laser is off and on, respectively. This normalized change is related to the change of the dielectric function [52]. In the low field limits, the dielectric function has the lorenzian form. The normalized change of the reflectivity coefficient can be expressed as [53]

$$\frac{\Delta R}{R} = \mathrm{Re}\left[\sum_{j=1}^{n} A_j e^{i\theta_j}\left(E - E_{cj} + i\Gamma_j\right)^{-m_j}\right] \tag{3.8}$$

where n is the number of features to be fitted. E is the photon energy. The A_j, θ_j, E_{cj} and Γ_j are parameters of the jth feature. A_j is the amplitude of the signal, θ_j is the phase respect to the modulating laser beam, E_{cj} is the transition energy and Γ_j is the broadening parameter. The parameter m is the line shape factor which depends on type of critical point. In the three-dimension system, m = 2.5 is used.

PR measurement was performed at Onabe Lab, University of Tokyo. The 488 nm-line of argon ion laser was employed as the modulating source. The Xenon lamp is the probing light source. The reflected light is detected by the Si photodetector. The PR set up is shown in Fig. 3.9.

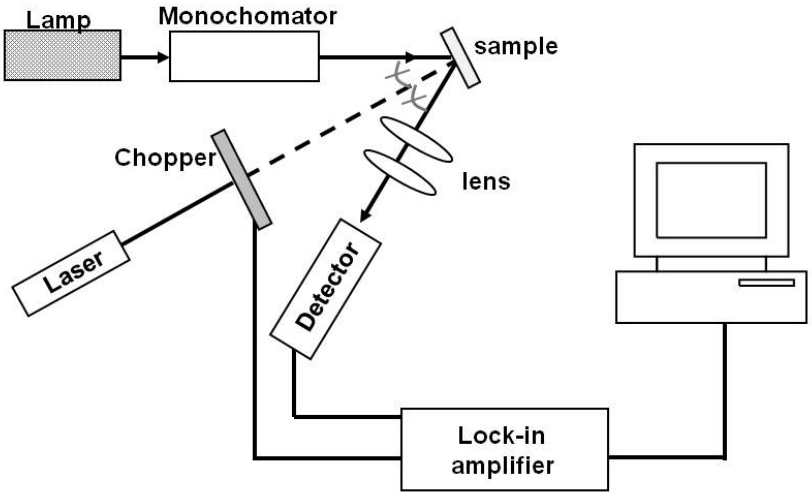

Figure 3.9: Schematic of PR set up

3.5 Raman scattering

When light incident to the sample, some fraction are scattered. There are two possible processes for light scattering. First process is elastic scattering or Rayleigh scattering. In this process, the scattered photons have the same energy as the incident photons. Second process is the inelastic scattering or Raman scattering which the scattered photons have the energy different from the incident photons due to phonon creation or annihilation. The Raman scattering is divided into two cases, anti-Stokes and Stokes scattering which the scattered photons have the energy larger and smaller than the incident photons, respectively. Typically, Stokes scattering is chosen to measure because of higher intensity. The graph obtained from measurement is plotted between the Raman shift (cm^{-1}) and the intensity of scattered photons. The Raman shift is defined by

$$\text{Raman shift } (\text{cm}^{-1}) \equiv \frac{1}{\lambda_{\text{incident}}} - \frac{1}{\lambda_{\text{scattered}}} \qquad (3.9)$$

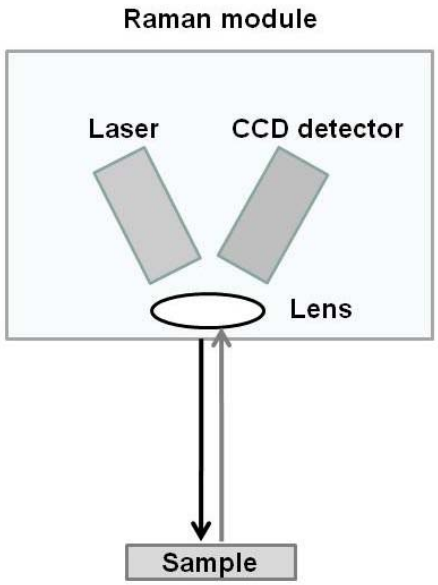

Figure 3.10: Schematic of Raman scattering measurement with back scattering geometry

where $\lambda_{incident}$ and $\lambda_{scattered}$ are the wavelength of the incident and scattered photons, respectively. This value is related to the phonon energies of bonds in the sample. The phonon temperature (Θ) can be calculated by the equation

$$\Theta = \frac{hc}{k_B}\left(\frac{1}{\lambda_{incident}} - \frac{1}{\lambda_{scattered}}\right) \quad (3.10)$$

where h is Planck's constant, c is the speed of light and k_B is Boltzmann's constant. The Raman pattern is the fingerprint of the material.

In this research, the Raman measurement with back scattering geometry was performed. The geometry is simple shown in Fig. 3.10. For ideal back scattering geometry, the Raman selection rule not allows the transverse phonon vibration mode.

The room temperature Raman measurement was performed at The Gem and Jewelry Institute of Thailand (Public Organization). The argon ion laser with wavelength 514.5 nm was used to the excitation source. The spot size of the laser beam is about 2 μm. the CCD detector is used.

CHAPTER IV

Results and discussion

The results and discussion of the dissertation are divided into 4 papers.

Beginning with **Paper I**, nearly lattice-matched $In_{0.528}Ga_{0.472}P_{0.973}N_{0.027}$/GaAs bulk, $In_{0.528}Ga_{0.472}P_{0.973}N_{0.027}$/GaAs QW and GaAs/$In_{0.528}Ga_{0.472}P_{0.973}N_{0.027}$ QW with higher N content were successfully grown by MOVPE. The results from HRXRD show the distinct Pendellösung fringes which indicate the high structural quality with flat interface and smooth surface. The 10K-PL spectra in a range of 1.4 - 2.0 eV show the red emission at 1.73 eV from $In_{0.528}Ga_{0.472}P_{0.973}N_{0.027}$ bulk and GaAs/$In_{0.528}Ga_{0.472}P_{0.973}N_{0.027}$ QW, but no such emission was observed for the $In_{0.528}Ga_{0.472}P_{0.973}N_{0.027}$/GaAs QW. This red emission is attributed to the emission from $In_{0.528}Ga_{0.472}P_{0.973}N_{0.027}$ alloy. The 10K-PL spectra in lower energy range of 1.0 - 1.6 eV show the extra peaks appear at energies of 1.357 and 1.351 eV for $In_{0.528}Ga_{0.472}P_{0.973}N_{0.027}$/GaAs QW and GaAs/$In_{0.528}Ga_{0.472}P_{0.973}N_{0.027}$ QW, respectively. These transitions are considered as an indirect transition between electrons located in the InGaPN and holes located in the GaAs regions. Temperature dependent PL results show that the extra peak of GaAs/$In_{0.528}Ga_{0.472}P_{0.973}N_{0.027}$ QW survives for the temperature up to 240K. On the other hand, the extra peak of $In_{0.528}Ga_{0.472}P_{0.973}N_{0.027}$/GaAs QW is completely quenched at the temperature about 120K. This situation suggested that both the $In_{0.528}Ga_{0.472}P_{0.973}N_{0.027}$/GaAs and GaAs/$In_{0.528}Ga_{0.472}P_{0.973}N_{0.027}$ QWs exhibits a type-II quantum structure. The valence band and conduction band offsets were approximated to be 450 and 160 meV, respectively.

In **Paper II**, the reciprocal maps of the reflection from (115) plane of bulk and QWs are shown to indicate the 100% strained epitaxy. The lattice-mismatch is less than 0.1%. The temperature dependent PR measurement was used to confirm the

bandgap variation of $In_{0.528}Ga_{0.472}P_{0.973}N_{0.027}$ bulk. The conduction and valence band offsets were approximated. The schematic energy band diagrams of both type-II $In_{0.528}Ga_{0.472}P_{0.973}N_{0.027}$/GaAs QWs were clearly illustrated with the valence band and conduction band offsets of 450 and 160 meV, respectively. The potential of the natural type-II band alignment between $In_xGa_{1-x}P_{1-y}N_y$ (x = 0.528, y = 0.027) and GaAs for separating electrons and holes in solar cells was proposed.

In **Paper III**, $In_{0.528}Ga_{0.472}P_{1-y}N_y$ (y = 0 - 0.027) layers on GaAs (001) substrate were coherently grown by MOVPE. The HRXRD results show all N containing samples have the flat surface. With incorporation of N into $In_{0.528}Ga_{0.472}P$, the bandgap at 10K is red-shifted as large as 110 meV for the highest N-containing layer (y = 0.027), indicating a large bandgap bowing. The temperature dependence PL results of all N containing samples show the S-shape behavior due to an association of the localization states. The near-band edge emissions are survived up to room temperature. The layers with a smooth surface and high crystal quality were obtained when the lattice-matching condition is optimized. Further, the temperature dependence of the bandgap energy becomes significantly weak with increasing N content.

In **Paper IV**, the $In_{0.528}Ga_{0.472}P_{1-y}N_y$ (y = 0 - 0.027) bulk layers on GaAs (001) substrates were further investigated. The PR results at room temperature show that the energy gap is decreased with increasing N. The temperature dependent PL results were fitted to the Varshni and single-oscillator models. The fitting parameters (Θ, β) obtained from Vashni and single-oscillator models of $In_{0.528}Ga_{0.472}P_{1-y}N_y$ samples tend to increase with increasing N. The values shift toward the III-nitride (i.e. GaN and InN) characteristic. In order to observe the bonds in samples, the unpolarized Raman scattering measurement at room temperature was performed. This Raman scattering results is the first report for $In_xGa_{1-x}P_{1-y}N_y$ samples grown by MOVPE. The Raman scattering results of $In_{0.528}Ga_{0.472}P_{1-y}N_y$ samples show the weak peaks which are close to the position of GaN-LO peak. This GaN-like characteristic suggests a larger contribution of Ga-N bonds over than In-N bonds in N-containing samples. These GaN bonds might be the origin of the less dependence on temperature property observed in $In_{0.528}Ga_{0.472}P_{1-y}N_y$.

In this dissertation, there are several results that are the first report for $In_xGa_{1-x}P_{1-y}N_y$ layer grown on GaAs (001) substrate by MOVPE. The $In_xGa_{1-x}P_{1-y}N_y$ layers with higher N content (up to y = 0.027) were successfully coherent grown on GaAs substrate. The $In_xGa_{1-x}P_{1-y}N_y$ layer can be grown with lattice-matching to GaAs. Moreover, the results from $In_{0.528}Ga_{0.472}P_{0.973}N_{0.027}$/GaAs bulk and QW samples confirm the type-II interface. In addition, the Raman scattering results show that $In_xGa_{1-x}P_{1-y}N_y$ layers contain Ga-N bonds over than In-N bonds. The relation between Ga-N bonds and the less temperature dependence property of bandgap observed in $In_xGa_{1-x}P_{1-y}N_y$ are first proposed.

Those properties of $In_xGa_{1-x}P_{1-y}N_y$ are advantageous for the absorber layer application in solar cell.

PAPER I

Photoluminescence Study of Type-II InGaPN/GaAs Quantum Wells

Dares Kaewket, Sakuntam Sanorpim, Sukkaneste Tungasmita, Ryuji Katayama and Kentaro Onabe

Published in
Journal of Nanoscience and Nanotechnology
Volume 10, Number 11, Pages 7154-7157 (2010).

Photoluminescence Study of Type-II InGaPN/GaAs Quantum Wells

Dares Kaewket[1], Sakuntam Sanorpim[1,2,*], Sukkaneste Tungasmita[1,2], Ryuji Katayama[3,4] and Kentaro Onabe[3]

[1]*Department of Physics, Faculty of Science, Chulalongkorn University, Bangkok, 10330 Thailand*

[2]*Center of Innovative Nanotechnology, Chulalongkorn University, Bangkok, 10330 Thailand*

[3]*Department of Advanced Materials Science, The University of Tokyo, Kashiwa, Chiba, 277-8561 Japan*

[4]*Institute for Materials Research (IMR), Tohoku University, Sendai, 980-8577 Japan*

* Corresponding author: e-mail sakuntam.s@chula.ac.th

Abstract

Nearly lattice-matched $In_{0.528}Ga_{0.472}P_{1-y}N_y$ bulk layer and $In_{0.528}Ga_{0.472}P_{1-y}N_y$/GaAs and GaAs/$In_{0.528}Ga_{0.472}P_{1-y}N_y$ quantum wells with higher N content, y = 0.027, were grown on GaAs (001) substrates by metalorganic vapor phase epitaxy. High-resolution x-ray diffraction results demonstrated the high quality of both the layer and quantum wells with fairly flat interfaces. Temperature dependent photoluminescence results showed that a near-band-edge emission is dominant in the bulk $In_{0.528}Ga_{0.472}P_{0.973}N_{0.027}$ layer, which at low temperature (T<100K) is associated with localized emissions centered at ~1.73 eV. Bandgap of $In_{0.528}Ga_{0.472}P_{0.973}N_{0.027}$ was examined to be 1.81 and 1.78 eV at 10K and room-temperature, respectively. Low temperature (10K)-photoluminescence spectrum obtained from the GaAs/$In_xGa_{1-x}P_{1-y}N_y$ quantum well also exhibited red emission at 1.73 eV attributed to the emission from

the InGaPN barrier. In addition, there are the extra weak peaks appear in a near-infrared energy range at 1.357 and 1.351 eV for $In_xGa_{1-x}P_{1-y}N_y$/GaAs and GaAs/$In_xGa_{1-x}P_{1-y}N_y$ quantum wells, respectively. Such optical transitions are considered as an indirect transition between electrons located in the InGaPN and holes located in the GaAs regions. This situation suggested that both the $In_{0.528}Ga_{0.472}P_{0.973}N_{0.027}$/GaAs and GaAs/$In_{0.528}Ga_{0.472}P_{0.973}N_{0.027}$ quantum wells exhibits a type-II quantum structure. This interpretation is justified when the valence and conduction band offsets of the type-II band alignment, which are relatively approximated to be 450 and 160 meV, are properly taken into account.

Keywords: InGaPN, quantum well, type-II, MOVPE, photoluminescence, valence band offset

1. Introduction

InGaPN is a novel quaternary material in the group of dilute III-V-nitride semiconductors that can be lattice-matched to the conventional substrates such as GaAs [1] and GaP [2]. Its potential applications conclude of optoelectronic and electronic devices such as light emitting diodes (LEDs), laser diodes (LDs) [3-4], heterojunction bipolar transistors [1] and solar cells [1]. It is known that an incorporation of a few percent of N into InGaPN [5-6] drastically reduces the bandgap energy due to the huge bandgap bowing commonly found in other III-V-N materials like GaAsN [7], and GaPN [8] and InGaAsN [9]. As a result, this material is expected to be “engineered semiconductor”, since both its bandgap and lattice parameter can be adjusted by controlling of the incorporation of In and N. However, due to the limit of the extreme immiscibility that is characteristic of the dilute III-V-N type alloys, it was found that the high quality InGaPN layer on GaAs with high N content is difficult to obtained [10].

Until now, there have been only few reports on InGaPN quantum structures which are important for device fabrication. Among of these, we previously contributed to the studies of structural and optical properties of lattice-matched $In_xGa_{1-x}P_{1-y}N_y$/GaP layers and quantum wells (QWs) with higher N contents up to

y = 0.071 grown by metalorganic vapor phase epitaxy (MOVPE) [11-13]. The results demonstrated that the conduction band offsets (ΔE_C) of our InGaPN/GaP QWs are as large as 270 – 490 meV, which is depended merely on the N incorporation. On the other hand, Y. G. Hong *et al*. [1] reported that the valence band offset (ΔE_V) was estimated to be about 97% of the total band gap difference between GaAs and InGaPN (x = 0.540, y = 0 – 0.023). J. S. Hwang *et al*. [14] and M. Izadifard *et al*. [15] revealed that, for N content (y) exceeds 0.005, band alignment of $In_xGa_{1-x}P_{1-y}N_y$/GaAs interfaces change from type-I to type-II transition due to the lowering of conduction band caused by an incorporation of N. However, photoluminescence (PL) from both the InGaPN bulk and InGaPN/GaAs QWs lattice-matched to GaAs still has not been achieved for higher N content.

In this work, firstly, nearly lattice-matched $In_{0.528}Ga_{0.472}P_{1-y}N_y$ bulk layer, $In_{0.528}Ga_{0.472}P_{1-y}N_y$/GaAs and GaAs/$In_{0.528}Ga_{0.472}P_{1-y}N_y$ QWs with higher N content, y = 0.027, were fabricated on GaAs (001) substrates by MOVPE. Then, we have focused on their structural characteristics and the N-induced luminescence property, which has not been analyzed comprehensively.

2. Experimental details

$In_{0.528}Ga_{0.472}P_{1-y}N_y$ bulk layer, $In_{0.528}Ga_{0.472}P_{1-y}N_y$/GaAs and GaAs/$In_{0.528}Ga_{0.472}P_{1-y}N_y$ QWs with higher N content, y = 0.027, were grown on GaAs (001) substrates by low-pressure (60 Torr) MOVPE with H_2 carrier gas. The precursors of In, Ga, P, As and N were trimethylindium (TMIn), trimethylgallium (TMGa), tertiarybutylphosphine (TBP), tertiarybutylarsine (TBAs) and dimethyhydrazine (DMHy), respectively. The InGaP(N) layers were grown with an identical growth condition. After the growth of a 0.1 μm-thick GaAs buffer layer at 650°C, InGaP(N) bulk layers or QW structures were grown at 520°C. DMHy flow rate was 1500 μmol/min. The growth time of bulk and well layers was 10 minutes and 10 seconds, respectively.

High resolution x-ray diffraction (HRXRD) was used to evaluate alloy composition (x, y) and crystal quality of the $In_xGa_{1-x}P_{1-y}N_y$ bulk layer and the interface quality of the QWs. Luminescence property was characterized using PL measurements in temperature range from 10 to 300K. The 488 nm-line of argon ion

laser was employed as an excitation source. The luminescence signal was dispersed by a 0.3 m single monochromator and detected by a InGaAs detector using a standard lock-in technique.

3. Results and discussion

Figures 1 shows (004) 2θ/ω-scan HRXRD patterns of all the N-containing samples as well as a calibration $In_{0.528}Ga_{0.472}P$ bulk layer, which was measured for calibration of In content. The distinct Pendellösung fringes indicate that all N-containing samples have high structural quality with fairly flat interface and smooth surface. The lattice-mismatch between the InGaPN layer and GaAs layer is less than 0.1%. This indicates that nearly lattice-matched $In_{0.528}Ga_{0.472}P_{0.973}N_{0.027}$ bulk layer and QWs with higher N content and fairly flat interfaces have been grown on the GaAs substrates via MOVPE.

Figure 2 shows 10K-PL spectra of $In_{0.528}Ga_{0.472}P_{0.973}N_{0.027}$ bulk, $In_{0.528}Ga_{0.472}P_{0.973}N_{0.027}$/GaAs and GaAs/$In_{0.528}Ga_{0.472}P_{0.973}N_{0.027}$ QWs. PL emission observed from all samples was divided into high energy (1.4 – 2.0 eV) and lower

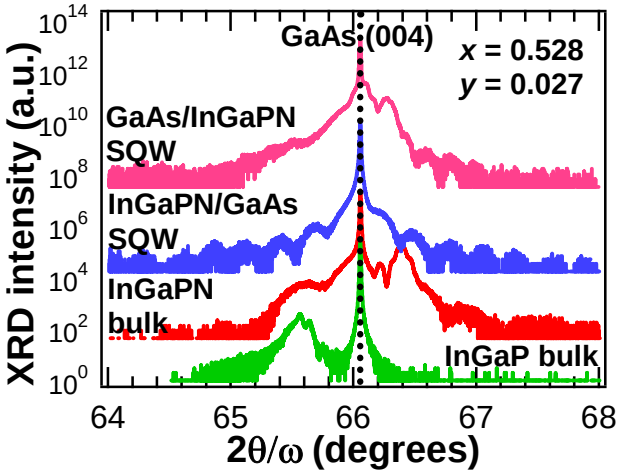

Figure 1: (004) 2θ/ω-scan HRXRD profiles of all samples as well as a calibration $In_{0.528}Ga_{0.472}P$ bulk layer

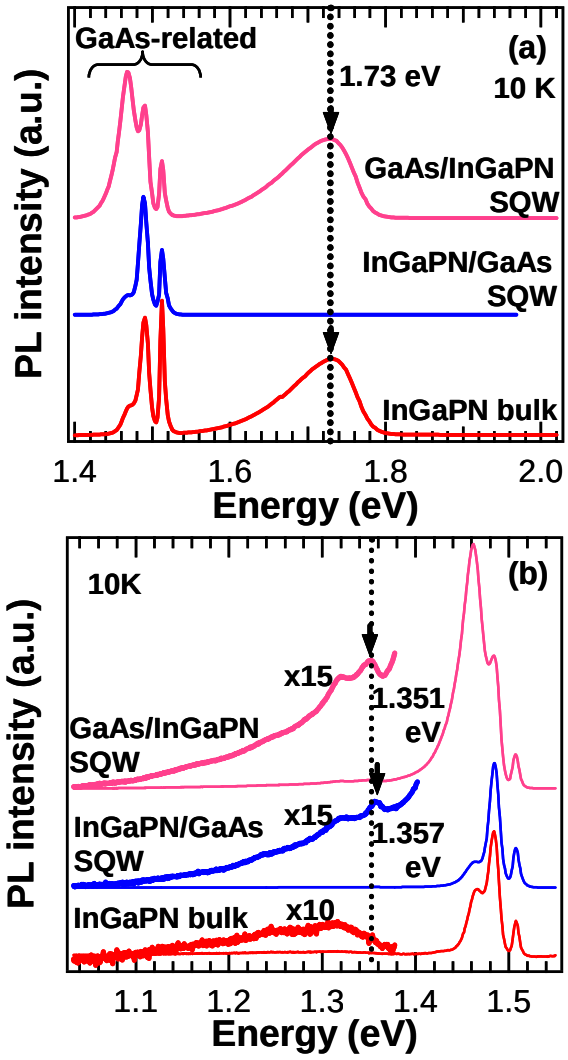

Figure 2: 10K-PL spectra of InGaPN bulk, InGaPN/GaAs QW and GaAs/InGaPN QW at (a) high energy (1.4 – 2.0 eV) and (b) lower energy (1.0 -1.6 eV) ranges

energy (1.0 -1.6 eV) ranges, as shown in Fig. 2(a) and Fig. 2(b), respectively. For PL spectra in high energy range, the group of GaAs-related peaks can be observed at energy position of 1.4 – 1.53 eV. In addition, the red emission at the energy of 1.73 eV was observed for $In_{0.528}Ga_{0.472}P_{0.973}N_{0.027}$ bulk and GaAs/$In_{0.528}Ga_{0.472}P_{0.973}N_{0.027}$ QW, but no such emission was observed for the $In_{0.528}Ga_{0.472}P_{0.973}N_{0.027}$/GaAs QW. The emission at 1.73 eV is attributed to the emission from InGaPN alloy. The bandtail

feature of the same PL spectra which emit from InGaPN layers was clearly observed. This long bandtail feature which observed in InGaPN and other dilute nitride semiconductors arises from alloy fluctuations induced by N [5, 16].

Figure 2(b) shows the 10K-PL spectra in lower energy range of 1.0-1.6 eV. PL spectrum of the $In_{0.528}Ga_{0.472}P_{0.973}N_{0.027}$ bulk exhibits broad PL band in energy range of 1.1 – 1.4 eV with intensity maximized at 1.31 eV. This may be due to a superposition between an additional a weak PL peak centered at 1.31 eV with the broad PL band. Such weak PL peak at 1.31 eV was also observed in PL spectra for all QWs. Besides this peak, an extra peak appears at higher energies of 1.357 and 1.351 eV for $In_{0.528}Ga_{0.472}P_{0.973}N_{0.027}$/GaAs QW and GaAs/$In_{0.528}Ga_{0.472}P_{0.973}N_{0.027}$ QW, respectively. Since the peak at 1.31 eV is found to locate at the same energy of all samples, thus, it should not relate to quantum confinement effect by the well. On the other hand, other two peaks at energy of 1.357 and 1.351 eV, which are emerged for the $In_{0.528}Ga_{0.472}P_{0.973}N_{0.027}$/GaAs and the GaAs/$In_{0.528}Ga_{0.472}P_{0.973}N_{0.027}$ QWs, respectively, is related to the sample's structure. As a result, these extra peaks are concern with quantum confinement effect by the well. It is known that for $In_xGa_{1-x}P_{1-y}N_y$/GaAs bulk samples with $y > 0.005$, the interface between InGaPN and GaAs is suggested to be a type-II interface [14-15], which showed an emission in the range of near infrared region. Consequently, the extra peak at 1.357 eV for the $In_{0.528}Ga_{0.472}P_{0.973}N_{0.027}$/GaAs QW should be considered as an indirect transition ($E_{PL\text{-}QW}$) between electrons located in the InGaPN and holes located in the GaAs regions. This situation suggested that both the $In_{0.528}Ga_{0.472}P_{0.973}N_{0.027}$/GaAs and GaAs/$In_{0.528}Ga_{0.472}P_{0.973}N_{0.027}$ QWs exhibits a type-II quantum structure.

To further understand such indirect transition observed from both QWs, temperature dependent PL of $In_{0.528}Ga_{0.472}P_{0.973}N_{0.027}$ bulk and QWs was performed. The PL peak energy is shown as a function of temperature in Fig. 3 for $In_{0.528}Ga_{0.472}P_{0.973}N_{0.027}$ bulk layer. The inset shows normalized PL spectra at different temperature (*T)*. At T=10K, only localized PL emission is observed. For T>100K, a new near-band-edge emission appears at an energy higher than localized PL emission and dominates up to room temperature with a significant intensity. We can assign the new PL band to free exciton recombination. The temperature dependence of PL peak energy can be fitted to Varshni relation [17] at the high temperature range (T=100-300K)

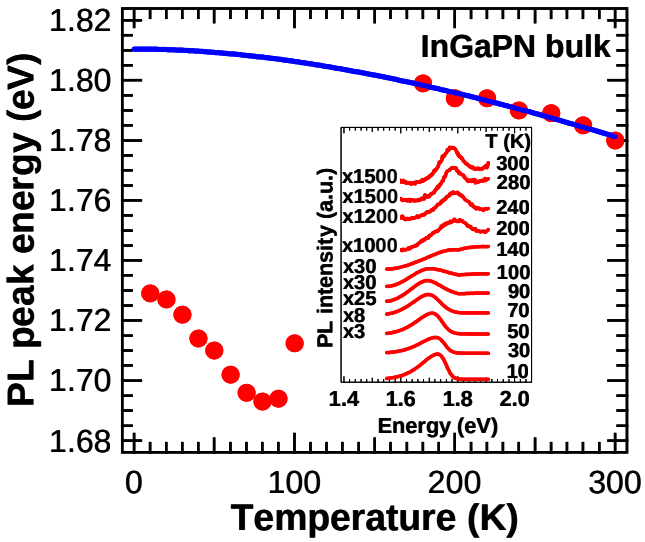

Figure 3: The position of PL main peak energy as a function of temperature (dotted line) and fitting line with Varshni's equation (solid line). The inset is temperature dependent PL spectra

with E_0= 1.811 eV, α = 0.266 meV/K and β = 505K (solid line). The temperature dependence in the lower temperature range shows an S shape phenomenon due to N related localized states, which normally observed in other III-V-N materials [18]. In addition, the localization energy at 10K, $\Delta E_{loc} = E_g(10K) - E_{PL}(10K)$, is estimated to be 80 meV. While, the bandgap at 10K obtained from the fitting is E_g = 1.811 eV.

Figures 4(a) and 4(b) respectively show normalized PL spectra in the lower energy range (1.2 -1.4 eV) of GaAs/$In_{0.528}Ga_{0.472}P_{0.973}N_{0.027}$ and $In_{0.528}Ga_{0.472}P_{0.973}N_{0.027}$/GaAs QWs with different temperatures. For GaAs/$In_{0.528}Ga_{0.472}P_{0.973}N_{0.027}$ QW, with increasing temperature, the $E_{PL\text{-}QW}$ peak at 1.351 eV is gradually shifts to lower energy due to the temperature induced bandgap reduction of both GaAs well and InGaPN barrier. This redshift is obviously seen when the temperature is higher than 140K. Surprisingly, this $E_{PL\text{-}QW}$ peak survives for the temperature up to 240K. On the other hand, the $E_{PL\text{-}QW}$ peak at 1.357 eV of the $In_{0.528}Ga_{0.472}P_{0.973}N_{0.027}$/GaAs QW (Fig. 4(b)) is completely quenched at the temperature about 120K. One possible

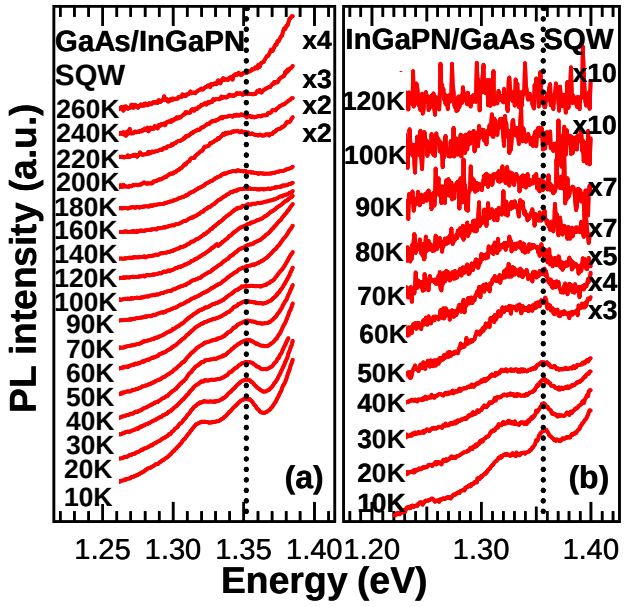

Figure 4: Temperature dependent PL spectra of (a) GaAs/$In_{0.528}Ga_{0.472}P_{0.973}N_{0.027}$ QW (b) $In_{0.528}Ga_{0.472}P_{0.973}N_{0.027}$/GaAs QW

explanation for this may be given in terms of thermal escaping of charge carriers from the quantum well with different barrier height.

It is expected that the most part of the bandgap reduction of $In_{0.528}Ga_{0.472}P_{0.973}N_{0.027}$ results from the lowering of conduction band [12, 14-15]. Correspondingly, the valence band offset as large as 450 meV at 10K can be estimated using "$\Delta E_V = E_{g,\text{-InGaPN}} - E_{\text{PL-QW}}$" for GaAs/InGaPN system. Thus, for GaAs well, valence band offset acts as a barrier height for holes confinement in the well. On the other hand, for the InGaPN well, the conduction band offset, which has calculated using "$\Delta E_C = E_{g,\ \text{GaAs}} - E_{\text{PL-QW}}$", is 160 meV acts as the barrier height for electrons confinement in the well. This evidence supports that the GaAs/$In_{0.528}Ga_{0.472}P_{0.973}N_{0.027}$ and $In_{0.528}Ga_{0.472}P_{0.973}N_{0.027}$/GaAs QWs are the type-II quantum structures.

4. Conclusion

Nearly lattice-matched $In_{0.528}Ga_{0.472}P_{0.973}N_{0.027}$/GaAs bulk, $In_{0.528}Ga_{0.472}P_{0.973}N_{0.027}$/GaAs and GaAs/$In_{0.528}Ga_{0.472}P_{0.973}N_{0.027}$ QWs with higher N content and flat interfaces were

successfully grown by MOVPE. Low temperature and temperature dependent PL spectra in near-infrared energy range of $In_xGa_{1-x}P_{1-y}N_y$/GaAs and GaAs/$In_xGa_{1-x}P_{1-y}N_y$ QWs exhibit an indirect transition between electrons located in the InGaPN and holes located in the GaAs regions. Our results suggest that, the GaAs/$In_xGa_{1-x}P_{1-y}N_y$ QW with the large valence band offset ΔE_V of 450 meV opens promising prospects for hole confinement in quantum device.

Acknowledgements

This work has been supported by Center of Innovative Nanotechnology under management of Chulalongkorn University. The work at the University of Tokyo was supported by NEDO of Japan. One of the authors (D. Kaewket) wishes to thank Thailand Research Fund through the Royal Golden Jubilee Ph.D. Program (Grant No. PHD/0090/2550) and The 90th Anniversary of Chulalongkorn University Fund for partial support of her work.

References

1. Y. G. Hong, R. André and C. W. Tu, J. Vac. Sci. Technol. B 19, 1413 (2001)
2. K. Onabe, T. Kimura, N. Nakadan, J. Wu, Y. Ito, S. Yoshida, J. Kikawa and Y. Shiraki, ICCG-13/ICVGE-11, Kyoto, 2001.
3. H. P. Xin, R. J. Welty, Y. G. Hong and C. W. Tu, J. Cryst. Growth 227-228, 558 (2001)
4. V. A. Odnoblyudov and C. W. Tu, Appl. Phys. Lett. 89, 191107 (2006)
5. Y. G. Hong, A. Nishikawa and C. W. Tu, Appl. Phys. Lett. 83, 26 (2003)
6. C. W. Tu, W. M. Chen, I. A. Buyanova and J. S. Hwang, J. Cryst. Growth 288, 7 (2006)
7. S. Sakai, Y. Ueta and Y. Terauchi, Jpn. J. Appl. Phys. 32, 4413 (1993)
8. J. N. Baillargeon, K. Y. Cheng, G. E. Hofler, P. J. Pearah and K. C. Hsieh, Appl. Phys. Lett. 60, 2540 (1992)
9. L. Bellaiche, Appl. Phys. Lett. 75, 2578 (1999)
10. S. Sanorpim, F. Nakajima, N. Nakadan, T. Kimura, R. Katayama and K. Onabe, J. Cryst. Growth 275, 1017 (2005)

11. D. Kaewket, S. Tungasmita, S. Sanorpim, F. Nakajima, N. Nakadan, T. Kimura, R. Katayama and K. Onabe, J. Cryst. Growth 298, 531 (2007)
12. D. Kaewket, S. Tungasmita, S. Sanorpim, R. Katayama and K. Onabe, Proceedings of the 2nd IEEE-NEMS 695 (2007)
13. D. Kaewket, S. Tungasmita, S. Sanorpim, R. Katayama and K. Onabe, Adv. Mater. Res. 55-57, 821 (2008)
14. J. S. Hwang, K. I. Lin, H. C. Lin, S. H. Hsu, K. C. Chen and Y. T. Lu, Appl. Phys. Lett. 86, 061103 (2005)
15. M. Izadifard, J. P. Bergman, W. M. Chen and I. A. Buyanova, Y. G. Hong and C. W. Tu, J. Appl. Phys. 99, 073515 (2006)
16. R. A. Mair, J. Y. Lin, and H. X. Jiang, E. D. Jones, A. A. Allerman and S. R. Kurtz, Appl. Phys. Lett. 76, 188 (2000)
17. Y. P. Varshni, Physica 34, 149 (1967)
18. S. Mazzucato, R.J. Potter, A. Erola, N. Balkan, P.R. Chalker, T.B. Joyce, T.J. Bullough, X. Marie, H. Carrere, E. Bedel,G. Lacoste, A. Arnoult and C. Fontaine, Physica E 17, 242 (2003)

PAPER II

Band Alignment of Lattice-matched InGaPN/GaAs and GaAs/InGaPN Quantum Wells Grown by MOVPE

Dares Kaewket, Sakuntam Sanorpim, Sukkaneste Tungasmita, Ryuji Katayama and Kentaro Onabe

Published in

Physica E: Low-dimensional Systems and Nanostructure

Volume 42, Pages 1176–1179 (2010).

Band Alignment of Lattice-matched InGaPN/GaAs and GaAs/InGaPN Quantum Wells Grown by MOVPE

Dares Kaewket[a], Sakuntam Sanorpim[a,*], Sukkaneste Tungasmita[a], Ryuji Katayama[b,c] and Kentaro Onabe[b]

[a]*Department of Physics, Faculty of Science, Chulalongkorn University, Phayathai Rd., Pathumwan, Bangkok, 10330 Thailand*

[b]*Department of Advanced Materials Science, The University of Tokyo, 5-1-5 Kashiwanoha, Kashiwa, Chiba, 277-8561 Japan*

[c]*Institute for Materials Research (IMR), Tohoku University, Sendai, 980-8577 Japan*

**Corresponding author (Sakuntam.S@chula.ac.th)*

Tel: +66-22187541

Fax: +66-22531150

Abstract

The band alignment of nearly lattice-matched $In_{0.528}Ga_{0.472}P_{1-y}N_y$/GaAs and GaAs/$In_{0.528}Ga_{0.472}P_{1-y}N_y$ quantum wells with N content of y = 0.027 on GaAs (001) substrates grown by metalorganic vapor phase epitaxy were studied using low-temperature and temperature dependent photoluminescence (PL). Low temperature (10K) PL shows the emission ($E_{PL,QW}$) in the infrared region which related to sample's structures. For GaAs/$In_{0.528}Ga_{0.472}P_{0.973}N_{0.027}$ QW, the $E_{PL,QW}$ emission was observed at temperature up to 260K. The results reveal that the $In_{0.528}Ga_{0.472}P_{0.973}N_{0.027}$/GaAs and GaAs/$In_{0.528}Ga_{0.472}P_{0.973}N_{0.027}$ quantum wells exhibit a type-II quantum structure. Valence band offset ΔE_V as large as 450 meV was estimated for GaAs/$In_{0.528}Ga_{0.472}P_{0.973}N_{0.027}$ quantum well while the conduction band offset ΔE_C was estimated to be 160 meV for $In_{0.528}Ga_{0.472}P_{0.973}N_{0.027}$/GaAs quantum well. This type-II quantum structures refer to the natural type-II band alignment between $In_xGa_{1-x}P_{1-y}N_y$ (x = 0.528, y = 0.027) and

GaAs, which is useful for separation electrons and holes in the electronic and photovoltaic applications.

Keywords: InGaPN, quantum well, type-II, MOVPE, photoluminescence, valence band offset

1. Introduction

Nitrogen containing III-III-V alloys have been studied due to many applications of these controllable semiconductors system. These alloys include the family of $In_xGa_{1-x}P_{1-y}N_y$ materials which provide over the broad range of compositions. The adjustable bandgap values and the useful lattice-matching conditions to various substrate materials such as GaAs [1] found in these alloys enable diverse type of devices, both optical and electronic [2-5]. The band alignment of two contact interface becomes crucial with those applications. The one approach to observe this effect is studying of quantum well (QW) structures which are simple for fabricating and understanding. However, it is difficult to obtain the high quality $In_xGa_{1-x}P_{1-y}N_y$ layer on GaAs with high N content ($y > 0.020$) due to the limit of the extreme immiscibility that is characteristic of the dilute III-III-V-N type alloys [6].

In particular, we have studied the band alignment of $In_{0.528}Ga_{0.472}P_{1-y}N_y$/GaAs and GaAs/$In_{0.528}Ga_{0.472}P_{1-y}N_y$ QWs with N content, y = 0.027, on GaAs (001) substrates fabricated by metalorganic vapor phase epitaxy (MOVPE). This paper summarizes the study and highlights the existing issue in the development of this alloy system in device applications.

2. Experimental details

$In_{0.528}Ga_{0.472}P_{1-y}N_y$ bulk layer, $In_{0.528}Ga_{0.472}P_{1-y}N_y$/GaAs and GaAs/$In_{0.528}Ga_{0.472}P_{1-y}N_y$ QWs with higher N content, y = 0.027, on GaAs (001) substrates were grown by low-pressure (60 Torr) MOVPE using trimethylindium (TMIn), trimethylgallium (TMGa), tertiarybutylphosphine (TBP), tertiarybutylarsine (TBAs) and dimethyhydrazine (DMHy). The growth conditions of InGaP(N) layer are identical for all samples. A 100-nm-thick GaAs buffer layer was first grown on the

substrate at 650°C, and then InGaP(N) bulk layer or QW structures were grown at 520°C. [DMHy] flow rate was 1500 μmol/min. For the QWs, the thickness of well and cap layers are 7 nm and 28 nm, respectively.

High resolution x-ray diffraction (HRXRD) was used to evaluate alloy composition (x, y) and crystal quality of the $In_xGa_{1-x}P_{1-y}N_y$ bulk layer and the interface quality of the QWs. The interband transitions of the QW structures were studied by temperature dependent photoluminescence (PL). The 488 nm-line of argon ion laser was employed as an excitation source. The luminescence signal was dispersed by a 0.3 m single monochromator and detected by an InGaAs detector (in infrared region) and a Si-photodetector (in visible region) for using a standard lock-in technique. The photoreflectance (PR) measurement was performed for the InGaPN bulk layer to determine the bandgap value. The argon ion laser and a Xe-lamp were used as a pumping beam and a probing beam, respectively.

3. Results and discussion

Shown in Fig. 1 are X-ray reciprocal space maps (RSM) obtained from (a) $In_{0.528}Ga_{0.472}P_{0.973}N_{0.027}$ bulk, (b) $In_{0.528}Ga_{0.472}P_{0.973}N_{0.027}$/GaAs QW and (c) GaAs/$In_{0.528}Ga_{0.472}P_{0.973}N_{0.027}$ QW. Diffraction data from (004) and (115) planes are used to obtain the in-plane "$a_{//}$" lattice parameter and out of plane "$a_{\perp}$" lattice parameter assuming tetragonal lattice distortion. The dashed line indicate conditions for 100% strained epitaxy on the (115) RSMs. Analysis of the (004) and (115) RSM data indicate that nearly lattice-matched $In_{0.528}Ga_{0.472}P_{0.973}N_{0.027}$ bulk layer and QWs with N content as high as 0.027 have successfully grown on the GaAs (001) substrates via MOVPE. The Pendellösung patterns indicate the fairy flat interface and smooth surface for all the samples. The lattice-mismatch between the InGaPN layer and GaAs layer is estimated to be less than 0.1%. It is known that the lattice-matched condition reduces the dangling bonds, which affect the band lineup due to potential spike at the interface [7], near the interface.

Verification of the band alignment of quantum well system was accomplished using spectroscopic PL measurements. The low-temperature (10K) PL data, as shown in Fig. 2(a), indicate that the desired target near band edge emission energies at 1.73

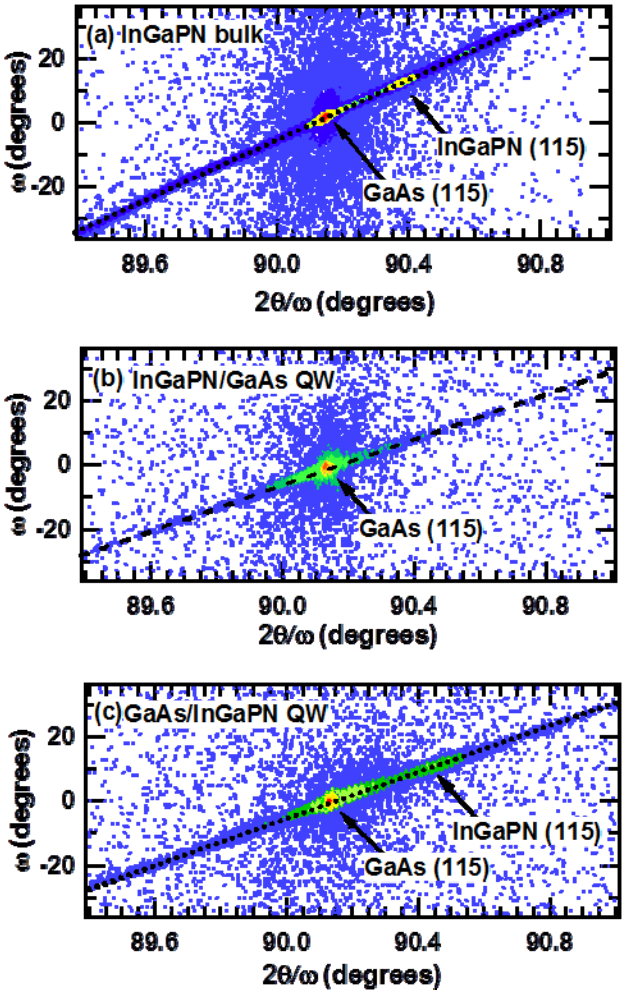

Figure 1: High resolution x-ray reciprocal space maps of (a) $In_{0.528}Ga_{0.472}P_{0.973}N_{0.027}$ bulk (b) $In_{0.528}Ga_{0.472}P_{0.973}N_{0.027}$/GaAs QW (c) GaAs/$In_{0.528}Ga_{0.472}P_{0.973}N_{0.027}$ QW obtained in the (115) sample orientations.

and 1.508 eV were obtained for $In_{0.528}Ga_{0.472}P_{0.973}N_{0.027}$ bulk layer and GaAs. Other GaAs-related emission was observed in the energy range of 1.4 – 1.5 eV. These emissions stay at the same position for all the samples. Moreover, there is also the near band edge emission located at energy of 1.73 eV for GaAs/$In_{0.528}Ga_{0.472}P_{0.973}N_{0.027}$ QW, but no such emission was observed for the $In_{0.528}Ga_{0.472}P_{0.973}N_{0.027}$/GaAs QW. It is expected that the bandgap value of $In_{0.528}Ga_{0.472}P_{0.973}N_{0.027}$ must exceed 1.73 eV and larger than bandgap of GaAs. For GaAs/$In_{0.528}Ga_{0.472}P_{0.973}N_{0.027}$ QW, except the

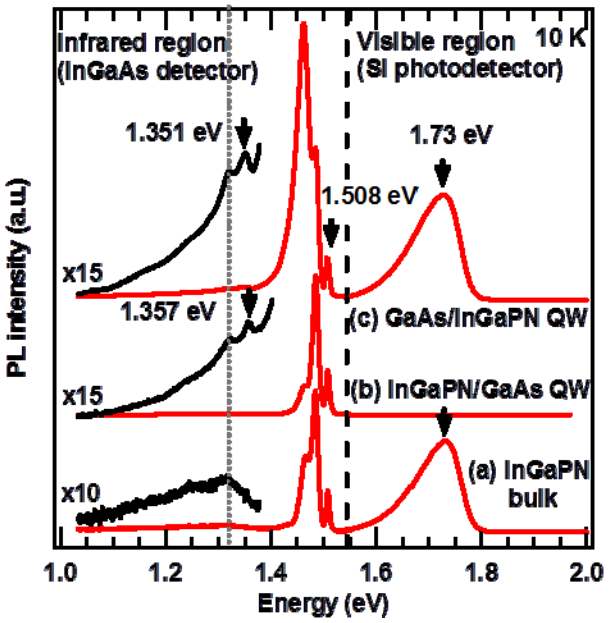

Figure 2: Low-temperature (10K) PL spectra obtained (a) $In_{0.528}Ga_{0.472}P_{0.973}N_{0.027}$ bulk, (b) $In_{0.528}Ga_{0.472}P_{0.973}N_{0.027}$/GaAs QW and (c) GaAs/$In_{0.528}Ga_{0.472}P_{0.973}N_{0.027}$ QW. Emission shown in infrared and visible regions, which are districted by dashed line, was detected using an InGaAs detector and a Si-photodetector, respectively.

peak at 1.73 eV, there is no PL emission appears at energy higher than energy gap of GaAs. This result suggests that no type-I quantum effect occurs in both the GaAs/$In_{0.528}Ga_{0.472}P_{0.973}N_{0.027}$ and $In_{0.528}Ga_{0.472}P_{0.973}N_{0.027}$/GaAs QWs.

Therefore, the emission of type-II transition, which is frequently observed in near-infrared region, is expected. For $In_{0.528}Ga_{0.472}P_{0.973}N_{0.027}$ bulk, the broad asymmetric feature at the energy around 1.1 – 1.4 eV can be observed with the maximum intensity centered at 1.32 eV as indicated by gray dashed line. For both QW samples, the weak PL peak at 1.32 eV can also be observed with smaller full width. As a result, in the case of bulk, this asymmetric broad feature may be due to a superposition between an additional a weak PL peak centered at 1.32 eV with the broad unknown PL band. Beside the weak peak at 1.32 eV, there is an extra peak appears at higher energies of 1.357 and 1.351 eV for $In_{0.528}Ga_{0.472}P_{0.973}N_{0.027}$/GaAs QW and GaAs/$In_{0.528}Ga_{0.472}P_{0.973}N_{0.027}$ QW, respectively. Since the peak at 1.32 eV is

found to locate at the same energy of both QWs and bulk layer, thus, it should not relate to quantum confinement effect by the well. On the other hand, other two peaks ($E_{PL,QW}$) at 1.357 and 1.351 eV, which are emerged for the $In_{0.528}Ga_{0.472}P_{0.973}N_{0.027}$/GaAs and the GaAs/$In_{0.528}Ga_{0.472}P_{0.973}N_{0.027}$ QWs, respectively, are concerned as a dependence of the sample's structures. Accordingly, as an expectation, these extra peaks are attributed to the quantum confinement effect by the well. This situation suggested that both the $In_{0.528}Ga_{0.472}P_{0.973}N_{0.027}$/GaAs and GaAs/$In_{0.528}Ga_{0.472}P_{0.973}N_{0.027}$ QWs exhibits a type-II quantum structure.

The temperature dependent PL of QWs was studied in a spectral range of near infrared. Figure 3 shows a typical temperature dependence of PL spectra obtained from GaAs/$In_{0.528}Ga_{0.472}P_{0.973}N_{0.027}$ QW. The PL spectrum at T = 10K can be

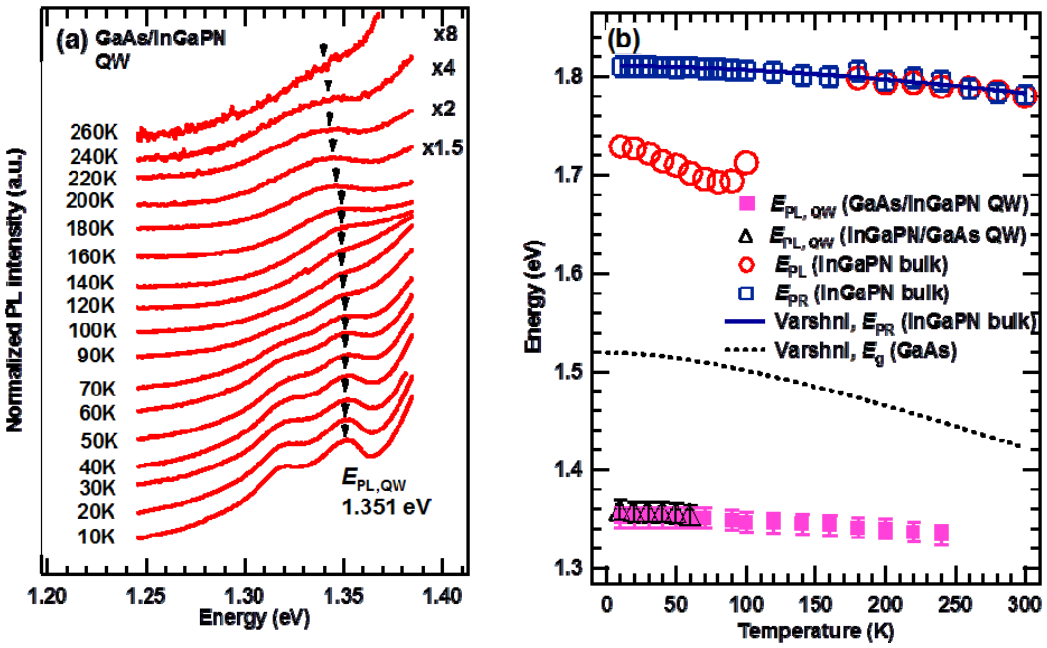

Figure 3: (a) Temperature dependent PL spectra of GaAs/$In_{0.528}Ga_{0.472}P_{0.973}N_{0.027}$ QW. (b) Temperature dependence of PL peak for GaAs/$In_{0.528}Ga_{0.472}P_{0.973}N_{0.027}$ QW, $In_{0.528}Ga_{0.472}P_{0.973}N_{0.027}$/GaAs QW, and $In_{0.528}Ga_{0.472}P_{0.973}N_{0.027}$ bulk. For comparison, temperature dependent PR peak position of $In_{0.528}Ga_{0.472}P_{0.973}N_{0.027}$ bulk as well as the bandgap energy of GaAs is also shown.

represented as a convolution of two emission bands, with the contribution of the interband transitions of GaAs/$In_{0.528}Ga_{0.472}P_{0.973}N_{0.027}$ QW ($E_{PL,QW}$) becoming predominant at high temperatures, from 90 up to 260K. The peak position of $E_{PL,QW}$ is gradually red-shifted with increasing temperature. On the other hand, the $E_{PL,QW}$ peak at 1.357 eV of the $In_{0.528}Ga_{0.472}P_{0.973}N_{0.027}$/GaAs QW (figure not shown) is suddenly quenched at the temperature about 60K. One possible explanation for difference in the quenching temperature may be given in terms of thermal escaping of charge carriers from the quantum well with different barrier height. This means that a strong quantum confinement effect (larger barrier high) is observed for the GaAs/$In_{0.528}Ga_{0.472}P_{0.973}N_{0.027}$ QW owing to a large valence band offset between the GaAs well and the $In_{0.528}Ga_{0.472}P_{0.973}N_{0.027}$ barrier.

To achieve a comprehensive understanding of the band alignment in InGaPN/GaAs QWs, temperature dependent PL and PR spectra of the $In_{0.528}Ga_{0.472}P_{0.973}N_{0.027}$ bulk were investigated to verify its bandgap and compare with $E_{PL,QW}$ values of QWs, as shown in Fig. 3(b). The Varshni fitted bandgap energy variation with temperature of GaAs from Ref. [8] was also plotted in the figure. The low temperature range (<180K) of PL data shows an S-shape phenomenon due to the N related localized states, which normally observed in other III-V-N materials [9]. At higher temperatures, the PL peak energy agrees well with the energy of PR peak position. The temperature dependence of bandgap of $In_{0.528}Ga_{0.472}P_{0.973}N_{0.027}$ was successfully approximated by Varshni's expression [10] with E_0= 1.810 eV, α = 0.300 meV/K and β = 693K. It is found that the value of $E_{PL,QW}$ is decreased with increasing temperature as a consequent of the bandgap variation. This confirms the transitions in quantum well structure which attribute to electrons recombine from conduction band of InGaPN down to holes in the well at valence band of GaAs. It should be noted that the type-II transition at the $In_xGa_{1-x}P_{1-y}N_y$/GaAs interface is found to maintain in the composition range $y > 0.005$ [1, 11-13].

To encourage this finding, the calculations of valence band offset (ΔE_V) and conduction band offset (ΔE_C) in both $In_{0.528}Ga_{0.472}P_{0.973}N_{0.027}$/GaAs and GaAs/$In_{0.528}Ga_{0.472}P_{0.973}N_{0.027}$ QWs have been performed using the 10K-PL and PR data in Fig. 3(b). The quantum confinement effect is not taken into account for this calculation because the energy level depends on the well depth (ΔE_V or ΔE_C) which is

unknown and we want to find. For the GaAs/$In_{0.528}Ga_{0.472}P_{0.973}N_{0.027}$ QW, the valence band offset ΔE_V for holes confinement in GaAs region as large as 450 meV was estimated using "$\Delta E_V = E_{g,InGaPN} - E_{PL,QW}$". On the other hand, for the $In_{0.528}Ga_{0.472}P_{0.973}N_{0.027}$/GaAs QW, the conduction band offset ΔE_C for electrons confinement in InGaPN region was estimated using "$\Delta E_C = E_{g,GaAs} - E_{PL,QW}$" and the value of ΔE_C = 160 meV is obtained. Because $E_{PL,QW}$ value includes the confinement energy, the actual values of both ΔE_V and ΔE_C should be larger than the estimated values. Based on these calculations, the energy band diagram of both type-II $In_{0.528}Ga_{0.472}P_{0.973}N_{0.027}$/GaAs and GaAs/$In_{0.528}Ga_{0.472}P_{0.973}N_{0.027}$ QWs is modeled as illustrated in Fig 4. The huge value of ΔE_V for holes confinement in the GaAs/$In_{0.528}Ga_{0.472}P_{0.973}N_{0.027}$ QW and the smaller value of ΔE_C for electrons confinement in the $In_{0.528}Ga_{0.472}P_{0.973}N_{0.027}$/GaAs QW cause the difference in the quenching temperature of $E_{PL,QW}$ (Fig. 3(a)).

We find out that the type-II InGaPN/GaAs quantum structures refer to the natural type-II band alignment between $In_xGa_{1-x}P_{1-y}N_y$ (x = 0.528, y = 0.027) and GaAs which opens promising prospects for many applications. The band structure shows the path for separating electrons and holes without a complicated design of the

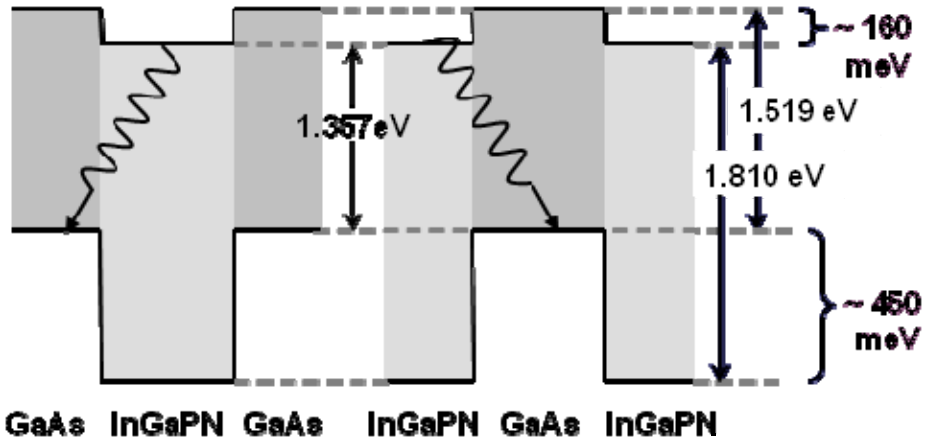

Figure 4: Schematic energy band diagram of the type-II $In_{0.528}Ga_{0.472}P_{0.973}N_{0.027}$/GaAs and GaAs/$In_{0.528}Ga_{0.472}P_{0.973}N_{0.027}$ QW structures

junction structure. Electrons flow into InGaPN region while holes flow into GaAs region. This is interesting for multijunction solar cells lattice-matched to GaAs or Ge substrates with two absorber layers, InGaPN and GaAs (or Ge). Moreover, it attracts the application for GaAs-based heterojunction bipolar transistors (HBTs). For emitter-base junction, the type-II band alignment with large valence band offset and small conduction band offset is more desirable. The large valence band offset improves the carrier injection efficiency and the current gain, while the small conduction band offset leads to the low-turn on voltage [14]. However, further works on ordering effect and electrical property are needed to be done.

4. Conclusion

Nearly lattice-matched $In_{0.528}Ga_{0.472}P_{0.973}N_{0.027}$ bulk, $In_{0.528}Ga_{0.472}P_{0.973}N_{0.027}$/GaAs and GaAs/$In_{0.528}Ga_{0.472}P_{0.973}N_{0.027}$ QWs with higher N content and flat interfaces were successfully grown by MOVPE. The $In_{0.528}Ga_{0.472}P_{0.973}N_{0.027}$/GaAs and GaAs/$In_{0.528}Ga_{0.472}P_{0.973}N_{0.027}$ QWs show a type-II transition of the band alignment. The main difference of bandgap is come from the valence band offset. The valence band and conduction band offsets were approximated to be 450 and 160 meV, respectively. This type-II quantum structures refer to the natural type-II band alignment between $In_xGa_{1-x}P_{1-y}N_y$ (x = 0.528, y = 0.027) and GaAs which is useful for separation of electrons and holes. This advantage opens promising prospects for tandem solar cells and HBTs.

Acknowledgements

The work at the University of Tokyo was supported by NEDO. One of the authors (D. Kaewket) wishes to thank Thailand Research Fund through the Royal Golden Jubilee Ph.D. Program (Grant No. PHD/0090/2550) and The 90th Anniversary of Chulalongkorn University Fund for partial support of her work.

References

[1] Y. G. Hong, R. André, C. W. Tu, Gas-source molecular beam expitaxy of GaInNP/GaAs and a study of its band lineup, J. Vac. Sci. Technol. B 19 (2001) 1413.

[2] H. P. Xin, R. J. Welty, Y. G. Hong, C. W. Tu, Gas-source MBE growth of Ga(In)NP/GaP structures and their applications for red light-emitting diodes, J. Cryst. Growth 227-228 (2001) 558.

[3] V. A. Odnoblyudov, C.W. Tu, Growth and fabrication of InGaNP-based yellow-red light emitting diodes, Appl. Phys. Lett. 89 (2006) 191107.

[4] J. Y. Duboz, M. Hugues, B. Damilano, A. Nedelcu, P. Bois, N. Kheirodin, F. H. Julien, Infrared detectors based on InGaAsN/GaAs intersubband transitions, Appl. Phys. Lett. 94 (2009) 022103.

[5] S. R. Kurtz, A. A. Allerman, E. D. Jones, J. M. Gee, J. J. Banas, B. E. Hammons, InGaAsN solar cells with 1.0 eV band gap, lattice matched to GaAs, Appl. Phys. Lett. 74, (1999) 729.

[6] M. Henini, Dilute nitride semiconductors, first ed., Elsevier, United Kingdom, 2005.

[7] B. L. Anderson, R. L. Anderson, Fundamentals of semiconductor devices, first ed., McGrow-Hill, New York, 2005.

[8] I. Vurgaftman, J. R. Meyer, L. R. Ram-Mohan, Band parameters for III-V compound semiconductors and their alloys, J. Appl. Phys. 89 (2001) 5815.

[9] S. Mazzucato, R.J. Potter, A. Erola, N. Balkan, P.R. Chalker, T.B. Joyce, T.J. Bullough, X. Marie, H. Carrere, E. Bedel,G. Lacoste, A. Arnoult, C. Fontaine, S-shaped behaviour of the temperature-dependent energy band gap in dilute nitrides, Physica E 17 (2003) 242.

[10] Y. P. Varshni, Temperature dependence of the energy gap in semiconductors, Physica 34 (1967) 149.

[11] J. S. Hwang, K. I. Lin, H. C. Lin, S. H. Hsu, K. C. Chen and Y. T. Lu, Studies of band alignment and two-dimensional electron gas in InGaPN/GaAs heterostructures, Appl. Phys. Lett. 86, 061103 (2005)

[12] M. Izadifard, T. Mtchedlidze, I. Vorona, W. M. Chen and I. A. Buyanova, Y. G. Hong and C. W. Tu, Band alignment in GaInNP/GaAs heterostructures grown by gas-source molecular-beam epitaxy, Appl. Phys. Lett. 86 (2005) 261904.

[13] M. Izadifard, J. P. Bergman, W. M. Chen and I. A. Buyanova, Y. G. Hong and C. W. Tu, Photoluminescence upconversion in GaInNP/GaAs heterostructures grown by gas source molecular beam epitaxy, J. Appl. Phys. 99 (2006) 073515.

[14] Q. J.Hartmann, D. A. Ahmari, Q. Yang, A. P. Curtis, G. E. Stillman, InGaP/GaAs carbon-doped heterostructures for heterojunction bipolar transistors, in: K. Kordoš, J. Norvák (Eds.), Heterostructure epitaxy and devices – HEAD'97, Kluwer academic publishers, Netherlands, 1998, pp. 155-160.

PAPER III

MOVPE Growth of High Optical Quality InGaPN Layers on GaAs (001) Substrates

Dares Kaewket, Sakuntam Sanorpim, Sukkaneste Tungasmita, Ryuji Katayama and Kentaro Onabe

Published in

Physica Status Solidi C

Volume 7, Issue 7 – 8, Pages 2079 – 2081 (2010).

MOVPE Growth of High Optical Quality InGaPN Layers on GaAs (001) Substrates

Dares Kaewket[*,1], Sakuntam Sanorpim[**,1], Sukkaneste Tungasmita[1], Ryuji Katayama[2,3] and Kentaro Onabe[2]

[1]*Department of Physics, Faculty of Science, Chulalongkorn University, Phayathai Rd., Bangkok, 10330, Thailand*

[2]*Department of Advanced Materials Science, The University of Tokyo, 5-1-5 Kashiwa, Chiba, 277-8561, Japan*

[3]*Institute for Materials Research (IMR), Tohoku University, Sendai, 980-8577, Japan*

Received 30 September 2009, revised 8 February 2010, accepted 15 February 2010
Published online 12 May 2010

* e-mail: dares_ka@yahoo.com, Phone: +66 89 159 7366, Fax: +66 2 253 1150
** Corresponding author: e-mail sakuntam.s@chula.ac.th, Phone: +66 2 218 7541, Fax: +66 2 253 1150

Abstract

Highly luminescent $In_{0.528}Ga_{0.472}P_{1-y}N_y$ layers (y = 0 – 0.027) were grown on GaAs (001) substrates by metalorganic vapor phase epitaxy. The dependence of photoluminescence (PL) properties on the N content in $In_{0.528}Ga_{0.472}P_{1-y}N_y$ layers was investigated. Near-band edge emissions were obviously observed up to room temperature. With increasing temperature, the PL peak energy exhibits an inverted S-shape, which explained by the strong localization of carriers at low-temperatures, while the band-to-band transition becomes dominant at higher temperatures. With incorporation of N into $In_{0.528}Ga_{0.472}P$, the bandgap at 10K is red-shifted as large as

110 meV for the highest N-containing layer (y = 0.027), indicating a large bandgap bowing. Further, the temperature dependence of the bandgap energy becomes significantly weak with increasing N content. Our results suggest that the density of states around the band edge of $In_{0.528}Ga_{0.472}P_{1-y}N_y$ is modified from that of $In_{0.528}Ga_{0.472}P$ due to the localized states possibly induced by the presence of N.

Keywords: InGaPN, MOVPE, photoluminescence, band gap, localization

1. Introduction

InGaPN is a quaternary alloy in the group of dilute nitride semiconductors. This alloy can be lattice-matched to GaAs [1] and GaP [2, 4]. It is known that the incorporation of a low content of N leads to a large reduction in bandgap energy, previously reported in InGaPN [3, 4]. The InGaPN alloy is expected to be "engineered semiconductor" since its bandgap energy and lattice parameter can be tuned by adjusting the In and N contents. The applications of InGaPN are like the host-material, InGaP, which provides wide applications of GaAs-based electronic devices, such as transistors and solar cells. However, the growth of a high N content InGaPN layer is still a challenge, since the N incorporation greatly induces degradation of the photoluminescence (PL) properties. Similar to the case of InGaAsN [5], the immiscibility between III-host and N atomic sizes cause the growing is difficult. Hence, the suitable and optimized growth conditions are required to reach the high quality epitaxial films. Therefore, the effect of N on the PL has to be verified to be able grow high optical quality InGaPN layer.

This work, we show that incorporation of a few percent of N in the $In_{0.528}Ga_{0.472}P$/GaAs layer grown by metalorganic vapour phase epitaxy (MOVPE) changes the temperature dependence of the PL spectrum significantly.

2. Experimental details

$In_{0.528}Ga_{0.472}P_{1-y}N_y$ (y = 0, 0.017, 0.021 and 0.027) layers were grown on GaAs (001) substrates by low-pressure (60 Torr) MOVPE using trimethylindium (TMI), trimethylgallium (TMG), tertiarybutylphosphine (TBP), tertiarybutylarsine (TBA) and

dimethylhydrazine (DMHy), as the precursors of In, Ga, P, As and N are respectively. After the growth of 0.1 μm-thick GaAs buffer layer at 650 °C, the $In_xGa_{1-x}P_{1-y}N_y$ layer was respectively grown at 520°C. H_2 is used as a carrier gas. [TMI]/III ratio was maintained at 0.63. In order to vary N content in the $In_xGa_{1-x}P_{1-y}N_y$ layer, the [DMHy] flow rates were varied between 0 – 1500 μmol/min. The surface morphologies of the grown layers are smooth and mirror like.

The In and N contents were determined by X-ray diffraction (XRD) reciprocal mapping measurements, in which the strain in the layer was taken into account [6]. The optical property was investigated by using low-temperature and temperature dependent (10 - 300K) PL. The argon ion laser was used as the excitation light source.

3. Results and discussion

Figure 1 illustrates typical (004) X-ray reciprocal space map (RSM) of the $In_{0.528}Ga_{0.472}P_{0.979}N_{0.021}$ layer lattice-matched to GaAs. The long surface-truncation rod, which seen for all our N-containing samples, is clearly observed. This feature is caused by the scattering from a very flat surface in the case of geometry that parallel to the substrate surface [6]. Although this streak makes the compositions are difficult to determine, it indicates the very flat surfaces of $In_{0.528}Ga_{0.472}P_{1-y}N_y$ layers. In addition, the (115) X-ray RSMs show that all layers were coherently grown with GaAs substrates.

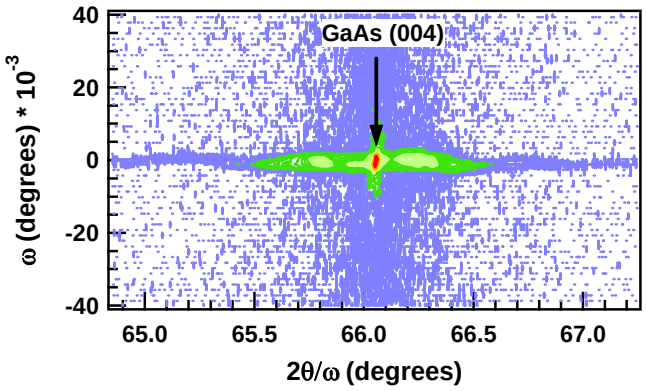

Figure 1: Typical (004) x-ray reciprocal space map of the $In_{0.528}Ga_{0.472}P_{0.979}N_{0.021}$ lattice-matched to GaAs

Typical 10K PL spectra of of all $In_{0.528}Ga_{0.472}P_{1-y}N_y$ samples (y = 0, 0.017, 0.021 and 0.027) grown with different [DMHy] flow rates, are shown in Fig. 2. The near-band edge PL emissions from $In_{0.528}Ga_{0.472}P$ layer with maximum at 1.918 eV and 1.896 eV have been established as free and bound excitons, respectively. With incorporation of N, the PL spectra with asymmetrical lineshape are shifted to a lower energy side due to the bandgap bowing. Comparing to the $In_{0.528}Ga_{0.472}P$, it is found that the red-shift is as large as 189 meV for the highest N-content $In_{0.528}Ga_{0.472}P_{0.973}N_{0.027}$ sample. PL spectrum shows the exponential tail at a low energy side while at a high energy side, it shows a sharp cut-off. These characteristic, which may be caused by the distribution of bandtail states, is commonly observed in other dilute-nitride materials [7] and also in InGaPN [3]. Besides, the PL line width (FWHM) of the N-containing $In_{0.528}Ga_{0.472}P_{1-y}N_y$ layers is broader than that of $In_{0.528}Ga_{0.472}P$ layer, this might due to the N incorporation. Nevertheless, the intensity of PL peaks emitted from our $In_{0.528}Ga_{0.472}P_{1-y}N_y$ layers is still high in comparison to the $In_{0.528}Ga_{0.472}P$ layer. Such high luminescence might refer to high crystal quality of InGaPN layers were grown on GaAs.

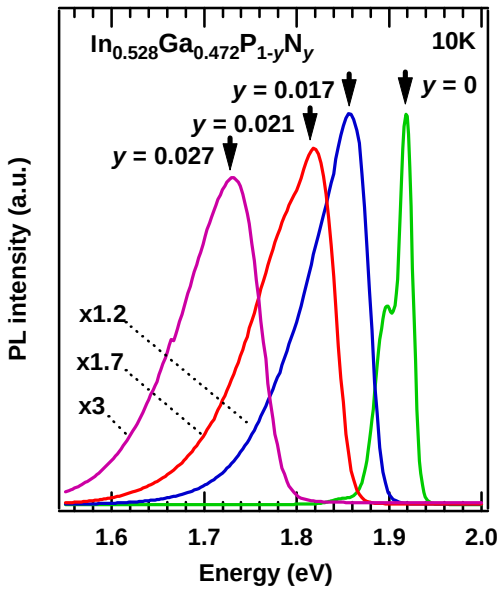

Figure 2: 10K-PL spectra of $In_{0.528}Ga_{0.472}P_{1-y}N_y$ layers with different N concentrations (y = 0 – 0.027). Arrows indicate the InGaPN-related emission.

Figure 3 shows the temperature dependence of PL spectra of $In_{0.528}Ga_{0.472}P_{0.979}N_{0.021}$ layer. At 10K, a distinct single peak (P_L) located at 1.818 eV is seen in the spectrum. It shifts to lower energies with increasing temperatures. Then, another peak (P_H) emerges at around 120 K. It is located at a higher-energy side of the peak P_L and becomes dominant at the higher temperatures. Further, the asymmetrical PL lineshape at the low temperatures (P_L) changes to higher symmetrical lineshape (P_H). This symmetrical emission P_H can be obviously observed up to room temperature.

The temperature dependence of the PL peak energies is plotted in Fig. 4. The main PL peak energies firstly red shifts then blue shifts and finally red shifts with temperatures. This might be considered as so-called "S-shape behaviour", which is typical of system having localized states [8]. As seen in the figure, P_L red shifts more rapidly than P_H with rise in temperatures. These results suggest that there exist two different origins of PL in InGaPN layers, namely localized (P_L) and free (P_H) excitonic recombination.

The Varshni's model [9] was employed to evaluate the effect of N on the bandgap of $In_{0.528}Ga_{0.472}P_{1-y}N_y$. The solid lines in Fig. 4 represent the expected change

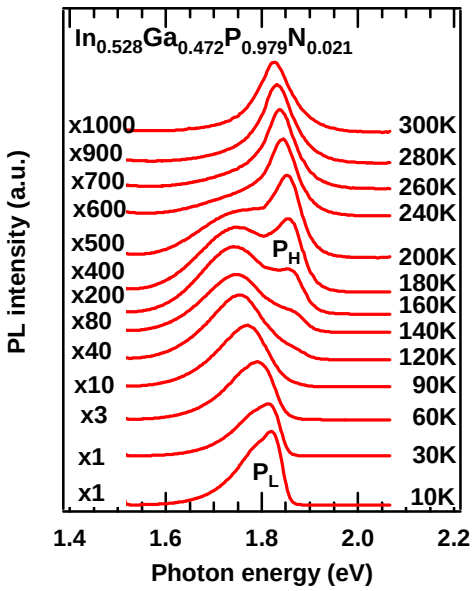

Figure 3: Temperature dependent PL spectra of $In_{0.528}Ga_{0.472}P_{0.979}N_{0.021}$ lattice-matched to GaAs.

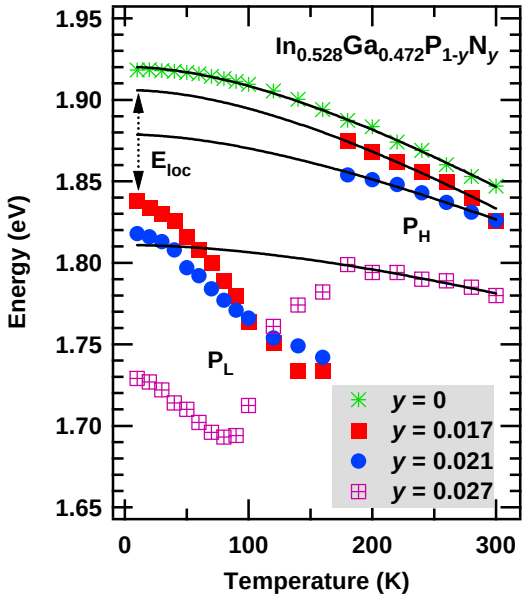

Figure 4: Main peak energies versus temperature of $In_{0.528}Ga_{0.472}P_{1-y}N_y$ layers with different N concentrations (y = 0 – 0.027). The solid lines are the fitting data with Varshni's model.

in the bandgap. The Varshni's fitting parameters and the localization energies at T = 10K ($E_{loc,10K}$ = E_g-P_L) and at the temperature that corresponding to the minimum energies of P_L ($E_{loc,max}$) are summarized in Table 1. The bandgap energies of $In_{0.528}Ga_{0.472}P_{1-y}N_y$ are less sensitive to temperature in comparison to that of $In_{0.528}Ga_{0.472}P$. For instance, the bandgap reduction from 10 to 300K rapidly decreases with incorporation of N. This rapid decrease of bandgap reduction is in good agreement with the results repoted by Uesugi et al. [10] and Yaguchi et al. [11].

4. Conclusion

MOVPE growth conditions were optimized for high-N containing $In_xGa_{1-x}P_{1-y}N_y$ layers on GaAs (001) substrates, and the bandgap and its temperature dependence of layers have been investigated by PL. The layers with a smooth surface and high crystal quality were obtained when the lattice-matching condition was optimized. Based on temperature dependence of PL, we have revealed two different origins of PL in $In_{0.528}Ga_{0.472}P_{1-y}N_y$ layers, exhibiting the S-shape behaviour due to an association of

the localization states. Namely, at low temperatures the N-induced localized states contribute to PL, while band-to-band transitions become dominant at higher temperatures. The near-band edge emissions are survived up to room temperature. For $In_{0.528}Ga_{0.472}P_{1-y}N_y$ with highest N content of $y = 0.027$, the bandgap reduction is as large as 110 meV in comparison to that of $In_{0.528}Ga_{0.472}P$. With an incorporation of N, the bandgap energies of $In_{0.528}Ga_{0.472}P_{1-y}N_y$ layers are less sensitive to temperature. These suggest that the density of states around the band edge of InGaPN is modified from that of InGaP due to the localized states possibly induced by the presence of N.

Acknowledgements

The work at the University of Tokyo was supported by NEDO. One of the authors (D. K) wishes to thank Thailand Research Fund through the Royal Golden Jubilee Ph.D. Program (Grant No. PHD/0090/2550) and The 90th Anniversary of Chulalongkorn University Fund for partial support of her work.

References

[1] Y. G. Hong, R. André and C. W. Tu, J. Vac. Sci. Technol. B **19**, 1413 (2001).

[2] K. Onabe, T. Kimura, N. Nakadan, J. Wu, Y. Ito, S. Yoshida, J. Kikawa and Y. Shiraki, presented in: ICCG-13/ICVGE-11, Kyoto (2001).

[3] C. W. Tu, W. M. Chen, I. A. Buyanova and J. S. Hwang, J. Cryst. Growth **288**, 7 (2006).

[4] D. Kaewket, S. Tungasmita, S. Sanorpim, R. Katayama and K. Onabe, Adv. Mater. Res. **55-57**, 821 (2008).

[5] M. Henini, Dilute nitride semiconductors (Elsevier, United Kingdom, 2005), p. 94.

[6] P. F. Fewster, X-ray Scattering from Semiconductors (Imperial College Press, London, 2003), p. 192, 255.

[7] I.A. Buyanova, W.M. Chen, C.W. Tu, Solid-State Electron. **47**, 467 (2003).

[8] S. Mazzucato, R.J. Potter, A. Erola, N. Balkan, P.R. Chalker, T.B. Joyce, T.J. Bullough, X. Marie, H. Carrere, E. Bedel,G. Lacoste, A. Arnoult and C. Fontaine, Physica E **17**, 242 (2003).

[9] Y. P. Varshni, Physica **34**, 149 (1967).

[10] K. Uesugi, I. Suemune, T. Hasegawa, T. Akutagawa, T. Nakayama, Appl. Phys. Lett. **76**, 1285 (2000).

[11] H. Yaguchi, S. Kikuchi, Y. Hijikata, S. Yoshida, D. Aoki, K. Onabe, Phys. Status Solidi (b) **228,** 273 (2001).

PAPER IV

Photoluminescence and Raman Scattering of InGaPN on GaAs

Dares Kaewket, Sakuntam Sanorpim, Sukkaneste Tungasmita, Ryuji Katayama and Kentaro Onabe

Manuscript

Photoluminescence and Raman Scattering of InGaPN on GaAs

Dares Kaewket[1], Sakuntam Sanorpim[*,1], Sukkaneste Tungasmita[1], Ryuji Katayama[2,3] and Kentaro Onabe[2]

[1]*Department of Physics, Faculty of Science, Chulalongkorn University, Phayathai Rd., Bangkok, 10330, Thailand*

[2]*Department of Advanced Materials Science, The University of Tokyo, 5-1-5 Kashiwa, Chiba, 277-8561, Japan*

[3]*Institute for Materials Research (IMR), Tohoku University, Sendai, 980-8577, Japan*

* Corresponding author: e-mail sakuntam.s@chula.ac.th

Abstract

$In_{0.528}Ga_{0.472}P_{1-y}N_y$ layers (y = 0 - 0.027) were coherently grown on GaAs (001) substrates by metalorganic vapor phase epitaxy. With incorporation of N into $In_{0.528}Ga_{0.472}P$, room temperature photoreflectance (PR) results show that the bandgap energies are significantly decreased. Temperature dependent PL peak energy of N-containing samples exhibited an inverted S-shape, which explained by strong localization at low-temperatures (<100K). Band-to-band transition becomes dominant at higher temperatures and was obviously observed up to room temperature. In addition, bandgap becomes less dependence on temperature with increasing N content. The Raman spectra of $In_{0.528}Ga_{0.472}P_{1-y}N_y$ show the GaN-like-LO peak at 738 cm^{-1} while the InN-LO peak is not observed. These results suggest that the Ga-N bonds make a larger contribution than In-N bonds in the $In_{0.528}Ga_{0.472}P_{1-y}N_y$ samples. The Ga-N bonds might be the origin of less dependence on temperature of bandgap energy in $In_{0.528}Ga_{0.472}P_{1-y}N_y$.

Keywords: InGaPN, MOVPE, photoluminescence, photoreflectance, raman scattering,

1. Introduction

InGaPN is a quaternary alloy in the group of dilute nitride semiconductors that can be lattice-matched to GaAs [1, 2] and GaP [3, 4]. It is known that the incorporation of a low content of N leads to a large reduction in bandgap energy, previously reported in InGaPN [4, 5]. Hence, InGaPN is the tuneable semiconductor that its bandgap energy and lattice parameter can be tuned by adjusting the In and N contents. InGaPN provides the potential for GaAs-based applications such as transistors and solar cells. However, the growth of a high N content InGaPN layer is still a challenge since the immiscibility between III-host and N atomic sizes which similar to the case of InGaAsN [6]. Hence, there are only few reports on InGaPN. The related parameters and the information of structural bonds are still required.

In this work, $In_{0.528}Ga_{0.472}P_{1-y}N_y$ layers (y = 0 - 0.027) were grown on GaAs (001) substrates by MOVPE. The small N incorporation into $In_{0.528}Ga_{0.472}P$ significantly modifies the temperature dependent PL spectra. The fitting with models was use to evaluate the bandgap and provide physical parameters. The Raman scattering was employed to observe the structural bonds in this material.

2. Experimental details

$In_{0.528}Ga_{0.472}P_{1-y}N_y$ (y = 0, 0.017, 0.021 and 0.027) layers were grown on GaAs (001) substrates by low-pressure (60 Torr) MOVPE using trimethylindium (TMI), trimethylgallium (TMG), tertiarybutylphosphine (TBP), tertiarybutylarsine (TBA) and dimethylhydrazine (DMHy), as the precursors of In, Ga, P, As and N are respectively. After the growth of GaAs buffer layer at 650 °C, the $In_xGa_{1-x}P_{1-y}N_y$ layer was respectively grown at 520°C. H_2 is used as a carrier gas. [TMI]/III ratio was maintained at 0.63. In order to vary N content in the $In_xGa_{1-x}P_{1-y}N_y$ layer, the [DMHy] flow rates were varied between 0 – 1500 μmol/min. The surface morphologies of the grown layers are smooth and mirror like. The In and N contents were determined by high resolution X-ray diffraction (HRXRD) reciprocal mapping measurements [1]. All layers were

coherently grown on GaAs substrates. The fundamental bandgaps at room temperature were determined by a standard arrangement of the photoreflectance (PR) apparatus. The 488 nm of argon ion laser was employed as the modulating source while the xenon lamp was used as the probing source. The transition of carriers and the variation of bandgap were investigated by the temperature dependent (10 - 300K) PL. The argon ion laser was used as an excitation light source. The unpolarized Raman spectroscopy was performed with backscattering geometry. The argon ion laser was used as the incident light source.

3. Results and discussion

In order to determine the fundamental bandgap, the PR measurement was performed. Figure 1 displays the PR spectra at room temperature of $In_{0.528}Ga_{0.472}P_{1-y}N_y$ samples (y = 0, 0.017, 0.021 and 0.027) samples. The PR results were fitted to [7]

$$\frac{\Delta R}{R} = \mathrm{Re}\left[\sum_{j=1}^{n} A_j e^{i\theta_j}\left(E - E_{cj} + i\Gamma_j\right)^{-m_j}\right] \quad (1)$$

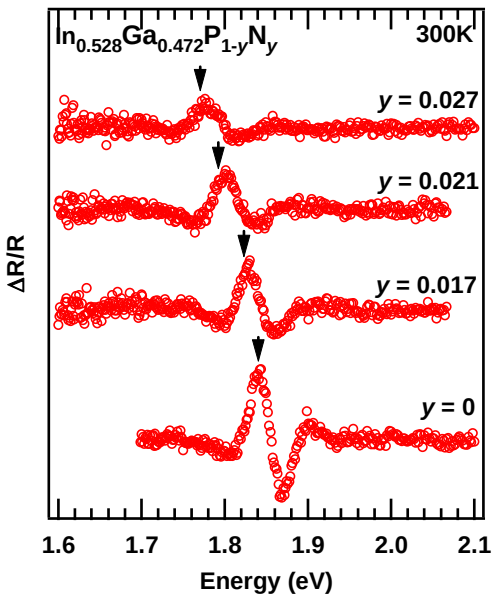

Figure 1: 300K PR spectra of $In_{0.528}Ga_{0.472}P_{1-y}N_y$ layers with different N concentrations (y = 0, 0.021 and 0.027). Arrows indicate the positions of bandgap energies obtained from the fitting.

where n is the number of features to be fitted. E is the photon energy. The A_j, θ_j, E_{cj} and Γ_j are the amplitude, phase, transition energy and broadening parameters of the jth feature, respectively. Here, m = 2.5 was used for three-dimensional critical point. In this work, in order to obtain only fundamental bandgap, the n = 1 was used. The bandgap energies obtained from the fitting of $In_{0.528}Ga_{0.472}P_{1-y}N_y$ with y = 0, 0.017, 0.021 and 0.027 are 1.841, 1.825, 1.795 and 1.773 eV, respectively. It is seen that the N incorporation into InGaP decrease the bandgap energy as previously found in other dilute nitride materials i.e. GaAsN [8-9] and InGaAsN [10].

In order to observe the variation of bandgap energy with temperature, the temperature dependant PL measurement was performed. Figure 2 shows the main peak energies versus temperature of $In_{0.528}Ga_{0.472}P_{1-y}N_y$ layers with various N concentrations (y = 0 – 0.027). The S-shape characteristic which often seen in dilute nitride alloys [11] is observed for all N-containing samples. This phenomena is believed that the carriers are trapped in N-related localize state before the recombination. The near-band-edge emissions of $In_{0.528}Ga_{0.472}P_{1-y}N_y$ samples can

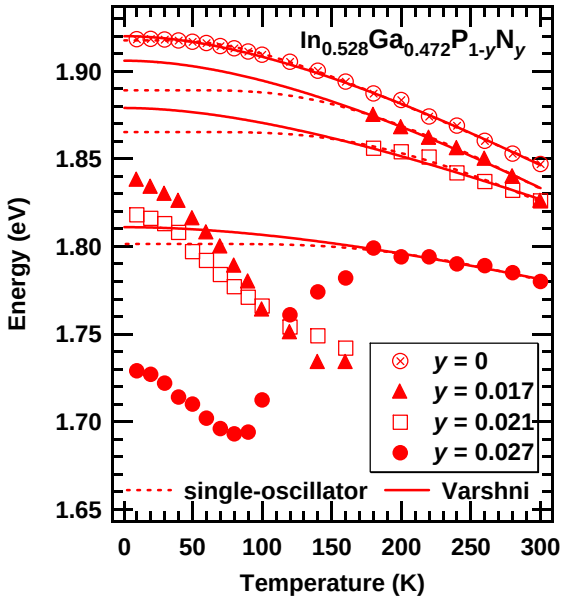

Figure 2: Main peak energies versus temperature of $In_{0.528}Ga_{0.472}P_{1-y}N_y$ layers with different N concentrations (y = 0 – 0.027). The solid lines correspond to the Varshni's model while the dash lines correspond to the single-oscillator model.

survive up to 300K. In order to evaluate the effect of N on the bandgap, the near-band-edge emissions were fitted with Varshni model [12] and single-oscillator model [13]. The empirical Varshni model is described by the equation;

$$E_g(T) = E_g(0) - \frac{\alpha T^2}{\beta + T} \tag{2}$$

where $E_g(T)$ is the bandgap at temperature T, $E_g(0)$ is the energy gap at 0K, α and β are the fitting constants. According to the single-oscillator model which equivalent to Bose-Einstein statistic, the temperature dependence of the bandgap can be given by

$$E_g(T) = E_g(0) - \frac{\gamma\Theta}{\exp(\Theta/T) - 1} \tag{3}$$

where γ and Θ are the fitting constants. The results obtained from the fitting procedure are shown in Table I. the fitting parameters were used to interpolate to lower temperature region which the localization is dominant. In point of view of the single-oscillator model, the γ is the limiting magnitude of the slope of the $E_g(T)$ curve in high-temperature. The Θ is average phonon temperature. By expanding the single-oscillator equation with Taylor series in case of $T>>\Theta$, these equation can be reduced to Varshni expression with $\gamma = \alpha$ and $\Theta = 2\beta$. From the fitting result, those fitting parameters obtained from two models are fair comparable. The deviation of fitted results obtained from two models in the low temperature region is arisen from the method of model [13] and lack of near-band-edge data in low temperature due to localization. With increasing N, the γ and α tend to decrease while the Θ and β tend to increase. The decreasing of slope in InGaPN samples indicates the variation of bandgap is less dependence on temperature in high-temperature range. The phonon temperature, Θ, is expected to relate with the Debye temperature [16]. The fitting results show that the Θ is increased with enhancing the N concentration. For the highest N containing samples, the Θ shows the value up to 756K. This larger Θ shifts toward the III-nitride semiconductors (i.e. GaN and InN) characteristic (see Table 1).

In order to examine the structural bond, the unpolarized Raman spectroscopy with back scattering geometry was performed. Figure 3 shows the Raman spectra in the range of Raman shift 50 – 900 cm^{-1} for $In_{0.528}Ga_{0.472}P$ and $In_{0.528}Ga_{0.472}P_{0.973}N_{0.027}$

material	$E_g(0)$ (eV)	α (meV/K)	β (K)	γ (meV/K)	Θ (K)
GaP	2.35 (2.339)	0.577	372	0.478	355
InP	1.424 (1.424)	0.363	162	0.396	272
GaN	3.299 (3.470)	0.593	600	0.614	587
InN	0.78 (1.994)	0.245	624	0.22	561
$In_{0.528}Ga_{0.472}P_{1-y}N_y$					
$y = 0$	1.920 (1.918)	0.536	355	0.379	265
$y = 0.017$	1.906 (1.889)	0.559	392	0.530	544
$y = 0.021$	1.879 (1.865)	0.365	330	0.496	671
$y = 0.027$	1.811 (1.801)	0.266	505	0.312	756

Table 1. Fitting parameters are obtained from Varshni and single-oscillator model. The $E_g(0)$ in the parentheses is obtained from single-oscillator model. The fitting values of binary compounds are obtained from Ref.[14-15] for Varshni model and from Ref.[16] for two-oscillator model. The fitting values of two-oscillator model in case of GaN and InN are obtained from hexagonal form.

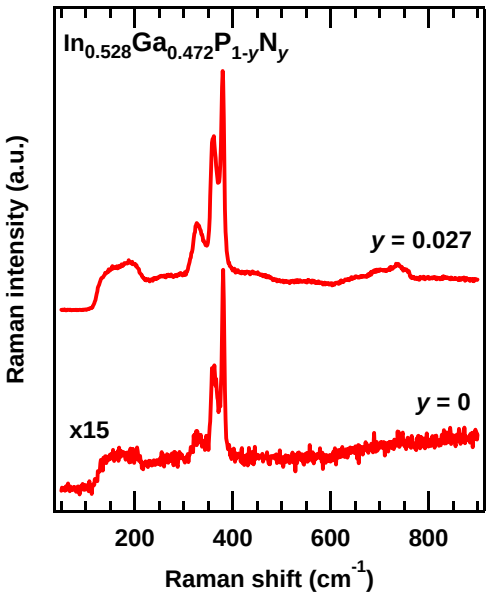

Figure 3: Main peak energies versus temperature of $In_{0.528}Ga_{0.472}P_{1-y}N_y$ layers with different N concentrations (y = 0 – 0.027). The solid lines correspond to the Varshni's model while the dash lines correspond to the single-oscillator model.

which are no-N and the highest N containing samples, respectively. The Raman spectra of $In_{0.528}Ga_{0.472}P_{0.973}N_{0.027}$ show higher intensity than $In_{0.528}Ga_{0.472}P$. For comparing, all range of Raman spectra were normalized with intensity of GaP-LO peak. For clearing view, the spectra of all samples are divided in 3 regions. Figure 4(a) shows the Raman spectra of all samples in the low region of 70 – 260 cm^{-1}. There is a broad feature at 110 – 220 cm^{-1} which related to the disorder-activated longitudinal acoustic phonons [17]. From the result, the feature of this broad peak in $In_{0.528}Ga_{0.472}P_{1-y}N_y$ is not much difference from InGaP. So, the N incorporation should not much perturb the crystal.

Figure 4(b) depicts the Raman spectra in 250 – 450 cm^{-1}. For InGaP, three well-known vibration modes in InGaP are observed. The peaks at 380, 360 and 328 cm^{-1} are correlated to GaP-LO, InP-LO and InP-TO phonons, respectively. For ideal back scattering geometry, the Raman selection rule not allows the transverse vibration mode. The appearance of this mode might arise from the small deviation of back scattering geometry and fluctuation in the alloy [17].

The Raman spectra in the region of 400-900 cm^{-1} are shown in Fig. 4(c). The group of peaks with dominant peak at 738 cm^{-1} is observed in $In_{0.528}Ga_{0.472}P_{1-y}N_y$ samples. This characteristic has also been discovered in InGaPN/GaAs grown by MBE [18]. The GaN-LO and GaN-TO phonon peaks of cubic GaN located at 742 and 555 cm^{-1} have been reported by H. Siegle *et al*. [19] while the InN-LO and InN-TO phonon peaks of cubic InN located at 586 and 472 cm^{-1} have been reported by G. Kaczmarczyk *et al* [20]. The dominant peak at 738 cm^{-1} is close to GaN-LO phonon. Moreover, there is a weak peak at 556 cm^{-1} which is close to GaN-TO phonon. However, there is no peak close to InN-LO or InN-TO phonon peaks. This phenomenon has been observed in c-InGaN [21]. Both LO and TO phonons of c-InGaN exhibit one-mode behavior that their frequencies linearly shift with alloy composition [22]. The group of LO phonon might be occur due to compositional fluctuation. Noticeable, the Raman spectra in the middle range (250 – 450 cm^{-1}) show the two-mode behavior similar to InGaP. Hence, the Raman mode of InGaPN might exhibit mixed behavior. Due to the Raman results of $In_{0.528}Ga_{0.472}P_{1-y}N_y$ samples show GaN-like characteristic, this suggests a larger contribution of Ga-N bonds over than In-N bonds in $In_{0.528}Ga_{0.472}P_{1-y}N_y$ samples. It can be interpreted that the N atoms

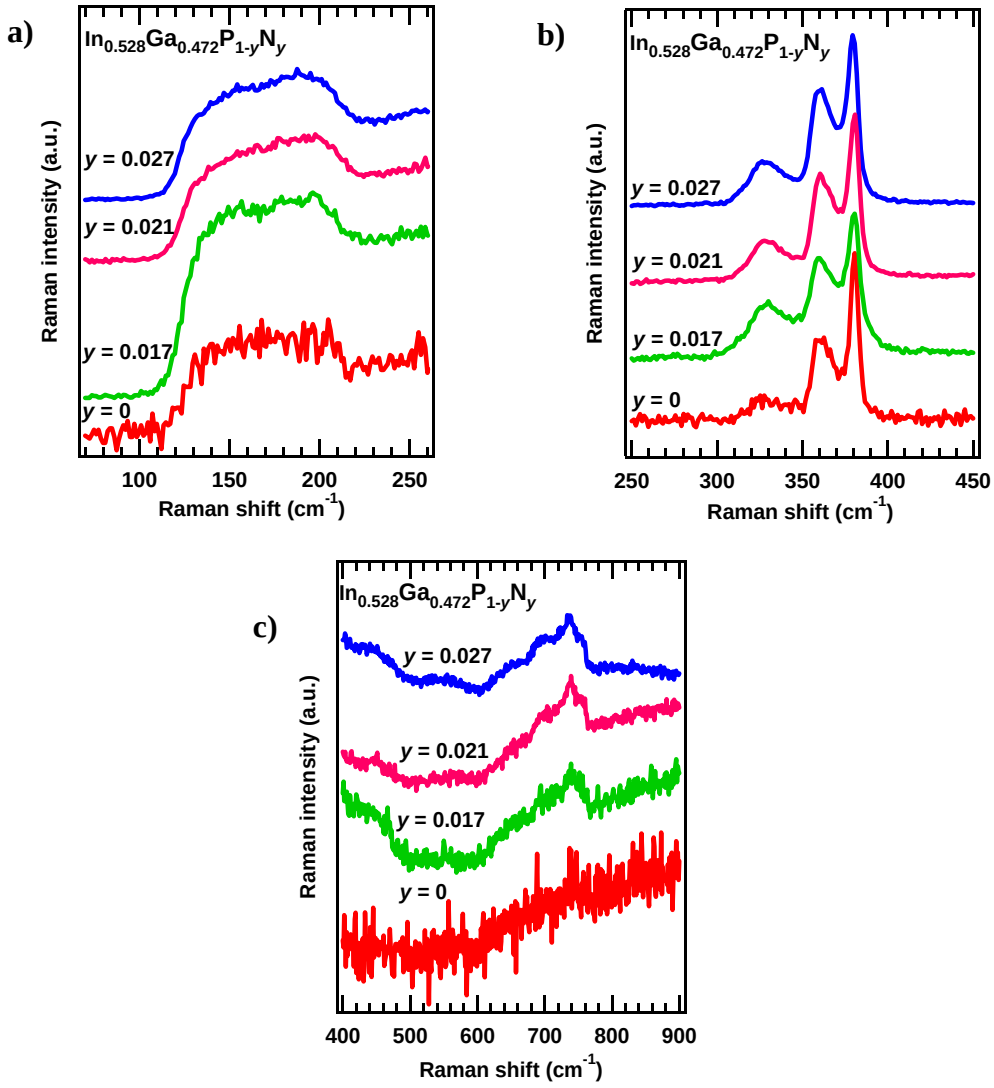

Figure 4: Raman spectra of $In_{0.528}Ga_{0.472}P_{1-y}N_y$ layers with different N concentrations (y = 0 – 0.027); (a) in the low wave number region, (b) in the middle wave number and (c) in the high wave number region.

prefer to bond with Ga atoms rather than In atoms which might be described by the relative weakness of the In-N bond compared to Ga-N [22]. According to the Raman peak, the related phonon temperature can be calculated. The phonon temperature related to Raman shift of InP-LO, GaP-LO and GaN-like-LO phonons are 518K, 547K and 1,062K, respectively. Comparing to fitted results from the temperature

dependent PL, the average phonon temperature, Θ, shift to higher temperature toward the GaN-like value.

From the above evidence, it is shown that the less dependence on temperature property is mostly contributed by Ga-N bonds. This Ga-N bonds might make InGaPN contains the advantage characteristics similar to GaN such as the high operating temperature and high radiation hardness [23]. Hence, InGaPN might open promising prospects for space solar cells and high operating temperature devices.

4. Conclusion

The $In_{0.528}Ga_{0.472}P_{1-y}N_y$ layers (y = 0 - 0.027) were coherently grown on GaAs (001) substrates by MOVPE. With incorporation of N, the bandgap energies are decreased. With increasing N, the PL peak exhibit red-shift which demonstrates the reduction of bandgap. The temperature dependent PL results show the S-shape characteristic which related to the strong localization of carriers. The bandgap becomes less dependence on temperature with increasing N content. From fitting the temperature dependent PL data with Varshni model and single-oscillator model, the β and Θ of $In_{0.528}Ga_{0.472}P_{1-y}N_y$ samples show the III-nitride (i.e. GaN and InN) characteristic. The Raman spectra of $In_{0.528}Ga_{0.472}P_{1-y}N_y$ show GaN-like-LO phonon mode. These results suggest that the Ga-N bonds make a larger contribution than In-N bonds in $In_{0.528}Ga_{0.472}P_{1-y}N_y$ samples. The less dependence on temperature property might be mostly contributed by Ga-N bonds.

Acknowledgements

The work at the University of Tokyo was supported by NEDO. One of the authors (D. K) wishes to thank Thailand Research Fund through the Royal Golden Jubilee Ph.D. Program (Grant No. PHD/0090/2550) and The 90th Anniversary of Chulalongkorn University Fund for partial support of her work.

References

[1] D. Kaewket, S. Sanorpim, S. Tungasmita, R. Katayama and K. Onabe, Phys. Status Solidi C **7**, 2079 (2010).

[2] Y. G. Hong, R. André and C. W. Tu, J. Vac. Sci. Technol. B **19**, 1413 (2001).

[3] K. Onabe, T. Kimura, N. Nakadan, J. Wu, Y. Ito, S. Yoshida, J. Kikawa and Y. Shiraki, presented in: ICCG-13/ICVGE-11, Kyoto (2001).

[4] D. Kaewket, S. Tungasmita, S. Sanorpim, R. Katayama and K. Onabe, Adv. Mater. Res. **55-57**, 821 (2008).

[5] C. W. Tu, W. M. Chen, I. A. Buyanova and J. S. Hwang, J. Cryst. Growth **288**, 7 (2006).

[6] M. Henini, Dilute nitride semiconductors (Elsevier, United Kingdom, 2005), p. 94.

[7] D.E. Aspnes, Surface Sci. **37,** 418 (1973).

[8] Sakai, S., Ueta, Y., and Terauchi, Y. J. Appl. Phys. **32**, 4413 (1993).

[9] J.Y. Duboz, J. A. Gupta, Z. R. Wasilewski, J. Ramsey, R. L. Williams, G. C. Aers, B. J. Riel and G. I. Sproule, Phys. Rev. B **66**, 85313 (2002).

[10] L. Bellaiche, Appl. Phys. Lett. 75, 2578 (1999).

[11] S. Mazzucato, R.J. Potter, A. Erola, N. Balkan, P.R. Chalker, T.B. Joyce, T.J. Bullough, X. Marie, H. Carrere, E. Bedel,G. Lacoste, A. Arnoult and C. Fontaine, Physica E **17**, 242 (2003).

[12] Y. P. Varshni, Physica **34**, 149 (1967).

[13] R. Pässler, E. Griebl, H. Riepl, G. Lautner, S. Bauer, H. Preis, W. Gebhardt, B. Buda, D. J. As, D. Schikora, K. Lischka, K. Papagelis and S. Ves, J. Appl. Phys. **86,** 4403 (1999).

[14] I. Vurgaftman, J. R. Meyer and L. R. Ram-Mohan, J. Appl. Phys. **89**, 5815 (2001).

[15] I. Vurgaftman and J. R. Meyer, J. Appl. Phys. **94**, 3675 (2003).

[16] R. Pässler, J. Appl. Phys. 89, 6235 (2001).

[17] H. M. Cheong, A. Mascarenhas, P. Ernst and C. Geng, Phys. Rev. B **56**, 1882 (1997).

[18] K. I. Lin, J. Y. Lee, T. S. Wang, S. H. Hsu, J. S. Hwang, Y. G. Hong and C. W. Tu, Appl. Phys. Lett. **86**, 211914 (2005).

[19] H. Siegle, L. Eckey, A. Hoffmann, C. Thomsen, B.K. Meyer, D. Schikora, M. Hankeln and K. Lischka, Solid State Commun. **96**, 943 (1995).

[20] G. Kaczmarczyk, A. Kaschner, S. Reich, A. Hoffmann, C. Thomsen, D. J. As, A. P. Lima, D. Schikora, K. Lischka, R. Averbeck and H. Riechert, Appl. Phys. Lett. **76**, 2122 (2000).

[21] E. Silveira, A. Tabata, J. R. Leite, R. Trentin, V. Lemos, T. Frey, D. J. As, D. Schikora and K. Lischka, Appl. Phys. Lett. **75**, 3602 (1999).

[22] H. Chen, R. M. Feenstra, J. E. Northrup, T. Zywietz and J. Neugebauer, Phys. Rev. Lett. **85**, 1902 (2000).

[23] S. M. Khanna, D. Estan, L. S. Erhardt, A. Houdayer, C. Carlone, A. Ionascut-Nedelcescu, S. R. Messenger, R. J. Walters, G. P. Summers, J. H. Warner and I. Jun, IEEE Trans. Nucl. Sci. **51**, 2729 (2004).

CHAPTER V

Conclusions

In this dissertation, the possibility of $In_xGa_{1-x}P_{1-y}N_y$ to use as the absorber layer in solar cell is studied. The samples studied in this work were grown by MOVPE growth method at Onabe Laboratory, University of Tokyo, Japan. In this dissertation, $In_{0.528}Ga_{0.472}P_{0.973}N_{0.027}$/GaAs and GaAs/$In_{0.528}Ga_{0.472}P_{0.973}N_{0.027}$ QWs were grown for investigating the band lineup between $In_{0.528}Ga_{0.472}P_{0.973}N_{0.027}$ and GaAs. In addition, the $In_{0.528}Ga_{0.472}P_{1-y}N_y$/GaAs bulk layers with various N concentrations (y = 0 - 0.027) were grown in order to investigate the effect of N incorporation to the structural and electronic properties. The properties of $In_xGa_{1-x}P_{1-y}N_y$ which are advantageous for solar cell applications are summarized as follows:

a) The incorporation of a low content of N into $In_xGa_{1-x}P$ leads to a reduction in bandgap energy. The $In_xGa_{1-x}P_{1-y}N_y$ layer can be grown with lattice-matching to GaAs. This is advantage for lattice-matched solar cell, especially multijunction solar cell.

b) There have been reported that the band alignment between $In_xGa_{1-x}P_{1-y}N_y$ (y > 0.005) and GaAs is type-II structure. It is confirmed in this research for $In_{0.528}Ga_{0.472}P_{0.973}N_{0.027}$/GaAs QWs with the large valence band offset of 450 meV. This natural type-II band structure shows the path for separating electrons and holes without a complicated design of the junction structure.

c) The localization states observed in the $In_xGa_{1-x}P_{1-y}N_y$ samples might be the potential for multiband solar cells.

d) The energy gap of $In_xGa_{1-x}P_{1-y}N_y$ is less sensitive to temperature with increasing N content. This property might be mostly contributed by Ga-N bonds. This property

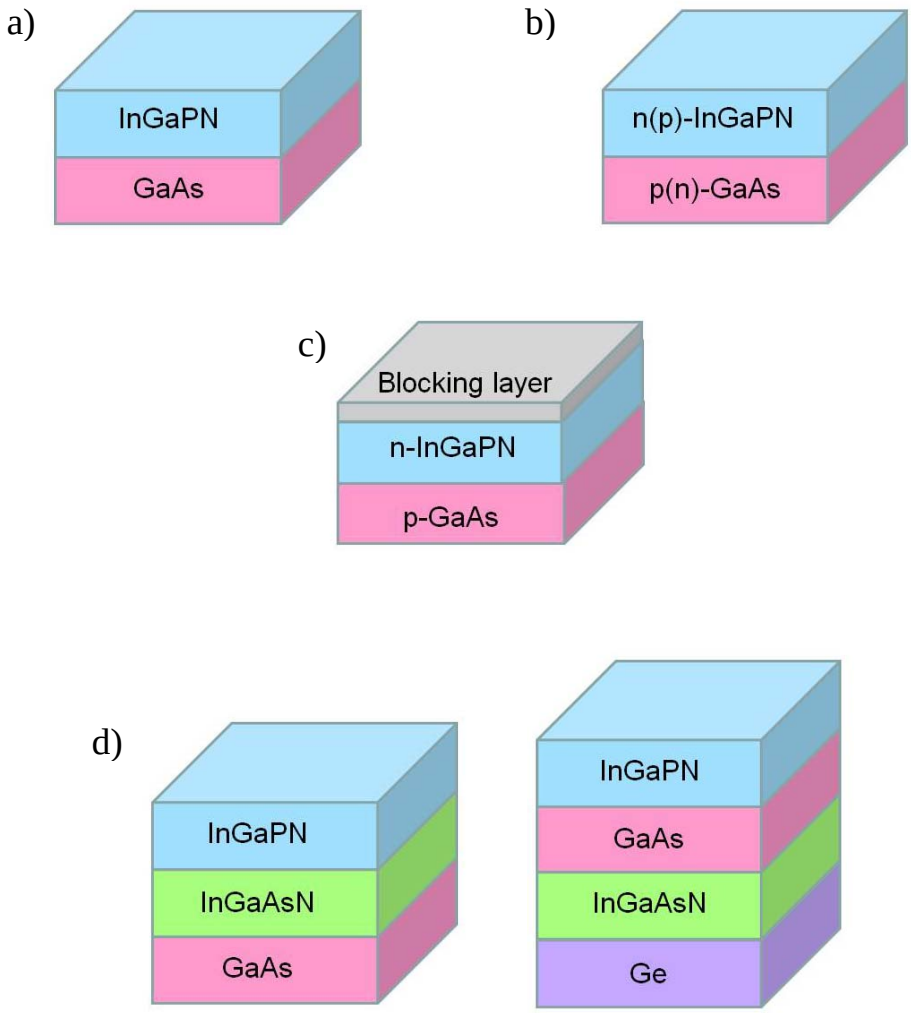

Figure 5.1: a) The simple two absorbers solar cell, InGaPN/GaAs, with natural type-II band alignment without doping, b) The two absorbers solar cell with doping, n(p)-InGaPN/p(n)-GaAs, in order to increase carrier concentration, c) The InGaPN multiband solar cell. The carriers from the intermediate band are isolated from the contact by the blocking layer in order to maintain the operation voltage which determined by the energy gap and d) The InGaPN/InGaAsN/GaAs and InGaPN/GaAs/InGaAsN/Ge lattice-matched multijunction solar cells, the energy gaps of InGaPN and InGaAsN are tunable (the details of doping and junction are not shown here)

might be the advantage for high-temperature operated solar cell. Moreover, the strong radiation hardness has been reported in GaN semiconductor, there is a possibility that $In_xGa_{1-x}P_{1-y}N_y$ might have the radiation hardness property which is superior to $In_xGa_{1-x}P$.

The possible simple structures are proposed in Fig. 5.1.

Suggestion from this dissertation (future work)

The $In_xGa_{1-x}P_{1-y}N_y$/GaAs samples with more In and N concentration should be grown and studied. The radiation hardness compared to InGaP should be examined. In addition, the electrical property of $In_xGa_{1-x}P_{1-y}N_y$, n-$In_xGa_{1-x}P_{1-y}N_y$ or p-$In_xGa_{1-x}P_{1-y}N_y$ should further be investigated.

REFERENCES

[1] Duboz, J.Y., et al. Band-gap energy of $In_xGa_{1-x}N_yAs_{1-y}$ as a function of N content. *Phys. Rev. B* 66 (2002) : 85313-85318.

[2] Kondow, M., Uomi, K., Niwa, A., Kitatani, T., Watahiki, S., and Yazawa, Y. GaInNAs: a novel material for long-wavelength-range laser diodes with excellent high-temperature performance. *Jpn. J. Appl. Phys*. 35 (1996) : 1273-1275.

[3] Kurtz, S.R., Allerman, A.A., Jones, E.D., Gee, J.M., Banas, J.J., and Hammons, B.E. InGaAsN solar cells with 1.0 eV band gap, lattice matched to GaAs. *Appl. Phys. Lett.* 74 (1999) : 729-731.

[4] Fischer, C. H., and Bhattacharya, P. Photoluminescence and deep levels in lattice-matched InGaAsN/GaAs. *J. Appl. Phys*. 96 (2004) : 4176-4180.

[5] Sanorpim, S., Nakajima, F., Ono, W., Katayama, R., and Onabe, K. High-nitrogen-content InGaAsN films on GaAs grown by metalorganic vapor phase epitaxy with TBAs and DMHy. *Phys. Status Solidi A* 203 (2006) : 1612-1617.

[6] Sanorpim, S., Nakajima, F., Katayama, R., Onabe, K., and Shiraki, Y. MOVPE growth and characterization of dilute $In_xGa_{1-x}As_{1-y}N_y$ on GaAs for 1 eV bandgap solar cell. *Asian J. Energy Environ*. 5 (2004) : 139-149.

[7] Uesugi, K., Kikuchi, T., Kuboya, S., Sanorpim, S., and Onabe, K. MOVPE growth of InGaAsN films on Ge(001) on-axis and vicinal substrates. *Phys. status solidi (c)* 9 (2012) : 542–545.

[8] Geisz, J.F., and Friedman, D.J. III–N–V semiconductors for solar photovoltaic applications. *Semicond. Sci. Technol*. 17 (2002) : 769-777.

[9] Green, M.A., Emery, K., Hishikawa, Y., Warta, W., and Dunlop, E.D. Solar cell efficiency tables (version 39). *Prog. Photovolt: Res. Appl*. 20 (2012) : 12-20.

[10] Gerhard, P., and Frank, D. Energy payback time of the high-concentration PV system FLATCON®. *Prog. Photovolt: Res. Appl*. 13 (2005) : 627-634.

[11] Bosi, M., and Pelosi, C. The potential of III-V semiconductors as terrestrial photovoltaic devices. *Prog. Photovolt: Res. Appl*. 15 (2007) : 51-68.

[12] Tu, C.W., and Yu, P.K.L. Material properties of III-V semiconductors for lasers and detectors. *MRS bulletin* May (2003) : 345-349.

[13] Green, M.A. *Third generation photovoltaics: advanced solar energy conversion*. Netherlands : Springer, 2003.

[14] Takamoto, T., Ikeda, E., Kurita, H., and Ohmori, M. Over 30% efficient InGaP/GaAs tandem solar cells. *Appl. Phys. Lett*. 70 (1997) : 381-383.

[15] Olson, J.M., Friedman, D.J., and Kurtz, S. High-efficiency III-V multijunction solar cells. In Luque, A., and Hegedus, S. (ed.), *Handbook of Photovoltaic Science and Engineering*, pp.359-411. United Kingdom : John Wiley & Sons, 2011.

[16] Geisz, J.F., and Friedman, D.J. III-N-V semiconductors for solar photovoltaic applications. *Semicond. Sci. Technol.* 17 (2002) : 769-777.

[17] Friedman, D.J., Geisz, J.F., Kurtz, S.R., and Olson, J.M. 1-eV solar cells with GaInNAs active layer. *J. Crystal Growth* 195 (1998) : 409-415.

[18] Kurtz, S., Friedman, D., Geisz, J., and McMahon, W. Using MOVPE growth to generate tomorrow's solar electricity. *J. Crystal Growth* 298 (2007): 748-753.

[19] Yoon, H., et al. Recent advances in high-efficiency III-V multi-junction solar cells for space applications: ultra triple junction qualification. *Prog. Photovolt: Res. Appl*. 13 (2005) : 133-139.

[20] Green, M.A. *Solar cells: operating principles, technology and system applications*. New Jersey : Prentice-Hall, 1992.

[21] Shockley, W., and Queisser, H.J. Detailed balance limit of efficiency of p-n junction solar cells. *J. Appl Phys*. 32 (1961) : 510-519.

[22] Würfel, P. *Physics of solar cells: from basic principles to advanced concepts*. Germany : Wiley-VCH, 2009.

[23] Bett, A.W., Dimroth, F., and Siefer, G. Multijunction concentrator solar cells. In Luque, A.L., and Andreev, V.M. (ed.), *Concentrator photovoltaics*, pp.67-87. Heidelberg : Springer, 2007.

[24] Hong, Y.G., André, R., and Tu, C.W. Gas-source molecular beam expitaxy of GaInNP/GaAs and a study of its band lineup. *J. Vac. Sci. Technol. B* 19 (2001) : 1413-1416.

[25] Onabe, K., et al. presented in: ICCG-13/ICVGE-11, Kyoto (2001).

[26] Xin, H.P., Welty, R.J., Hong, Y.G., and Tu, C.W. Gas-source MBE growth of Ga(In)NP/GaP structures and their applications for red light-emitting diodes. *J. Cryst. Growth* 558 (2001) : 227-228.

[27] Odnoblyudov, V.A., and Tu, C.W. Growth and fabrication of InGaNP-based yellow-red light emitting diodes. *Appl. Phys. Lett*. 89 (2006) : 191107-191109.

[28] Hong, Y.G., Nishikawa, A., and Tu, C.W. Effect of nitrogen on the optical and transport properties of $Ga_{0.48}In_{0.52}N_yP_{1-y}$ grown on GaAs(001) substrates. *Appl. Phys. Lett*. 83 (2003) : 5446-5448.

[29] Tu, C.W., Chen, W.M., Buyanova, I.A., and Hwang, J.S. Material properties of dilute nitrides: Ga(In)NAs and Ga(In)NP. *J. Cryst. Growth* 288 (2006) : 7-11.

[30] Sakai, S., Ueta, Y., and Terauchi, Y. Band gap energy and band lineup of III-V alloy semiconductors incorporating nitrogen and boron. *J. Appl. Phys*. 32 (1993) : 4413-4417.

[31] Baillargeon, J.N., Cheng, K.Y., Hofler, G.E., Pearah, P.J., and Hsieh, K. C. Luminescence quenching and the formation of the $GaP_{1-x}N_x$ alloy in GaP with increasing nitrogen content. *Appl. Phys. Lett*. 60 (1992) : 2540-2542.

[32] Bellaiche, L. Band gaps of lattice-matched (Ga,In)(As,N) alloys. *Appl. Phys. Lett*. 75 (1999) : 2578-2580.

[33] Shan, W., et al. Band anticrossing in GaInNAs alloys. *Phys. Rev. Lett*. 82 (1999) : 1221-1224

[34] Walukiewicz, W., et al. Interaction of localized electronic states with the conduction band: band anticrossing in II-VI semiconductor ternaries. *Phys. Rev. Lett*. 85 (2000) : 1552-1555

[35] Buyanova, I.A., and Chen, W.M. Optical and electronic properties of GaInNP alloys: a new material for lattice matching to GaAs. In Erol, A. (ed.),

Dilute III-V nitride semiconductors and material systems: physics and technology. Heidelberg : Springer, 2008.

[36] Buyanova, I.A., Izadifard, M., Chen, W.M., Hong, Y.G., and Tu, C.W. Modeling of band gap properties of GaInNP alloys lattice matched to GaAs. *Appl. Phys. Lett*. 88 (2006) : 031907.

[37] Lin, K.I., Wang, T.S., Tsai, J.T., and Hwang, J.S. Temperature-dependent parameters of band anticrossing in InGaPN alloys. *J. Appl. Phys*. 104 (2008) : 016109.

[38] Lin, K.I., Lin, H.C., Wang, T.S., Lee, M.H., Hwang, J.S. Analysis of band anticrossing in InGaPN alloys grown on GaAs substrates. *Phys. Status Solidi C* 5 (2008) : 449-453.

[39] Friedman, D.J., Geisz, J.F., and Ptak, A.J. Photovoltaic applications of dilute nitrides. In Buyanova, I.A., and Chen, W.M. (ed.), *Physics and applications of dilute nitrides*. Great Britain : Taylor & Francis Books, 2004.

[40] King, R.R., Sherif, R.A., Fetzer, C.M., and Colter, P. C. Advances in high-efficiency multijunction terrestrial concentrator cells and receivers. *Proc. Of NCPV and Solar Program Review Meeting* (2003) : 11.

[41] Luque, A., and Martí, A. Increasing the efficiency of ideal solar cells by photon induced transitions at intermediate levels. *Phys. Rev. Lett*. 78 (1997) : 5014–5017.

[42] Luque, A., Martí, A., Antolín, E., and Tablero, C. Intermediate bands versus levels in non-radiative recombination. *Physica B* 382 (2006) : 320-327.

[43] López, N., Reichertz, L.A., Yu, K.M., Campman, K., and Walukiewicz, W. Engineering the electronic band structure for multiband solar cells. *Phys. Rev. Lett*. 106 (2011) : 028701.

[44] Friedman, D.J., Geisz, J.F., Kurtz, S.R., Olson, J.M. 1-eV solar cells with GaInNAs active layer. *J. Cryst. Growth* 195 (1998) : 409-415.

[45] Zilko, J.L. Metal Organic Chemical Vapor Deposition: Technology and Equipment. In Seshan, K. (ed.), *Handbook of Thin Film Deposition*, pp.151-203. Great Britain : Elsevier, 2012.

[46] Yu, K.M., et al. Energetic Beam Synthesis of Dilute Nitrides and Related Alloys. In Erol, A. (ed.), *Dilute III-V Nitride Semiconductors and Material Systems: Physics and Technology*, pp.1-34. Heidelberg : Springer, 2007.

[47] Varshni, Y. P. Temperature dependence of the energy gap in semiconductors. *Physica* 34 (1967) : 149-154.

[48] Viña, L., Logothetidis, S., and Cardona, M. Temperature dependence of the dielectric function of germanium. *Phys. Rev. B* 30, (1984) : 1979-1991.

[49] Pässler, R. Basic Model Relations for Temperature dependencies of fundamental energy gaps in semiconductors. *Phys. Status Solidi B* 200, (1997) : 155-172.

[50] Pässler, R., et al. Temperature dependence of exciton peak energies in ZnS, ZnSe, and ZnTe epitaxial films. *J. Appl. Phys*. 86, (1999) : 4403-4411.

[51] Mazzucato, S., et al. S-shaped behaviour of the temperature-dependent energy band gap in dilute nitrides. *Physica E* 17, (2003) : 242-244.

[52] Seraphin, B. O., and Bottka, N. Band-structure analysis from electro-reflectance studies. *Phys. Rev*., 145 (1966) : 628-636.

[53] Aspnes, D.E. The analysis of optical spectra by Fourier methods. *Surface Sci*., 37 (1973) : 418-442.

APPENDIX

APPENDIX

Publications and presentations

1. Publications

[1] **D. Kaewket**, S. Sanorpim, S. Tungasmita, R. Katayama and K. Onabe, "Band alignment of lattice-matched InGaPN/GaAs and GaAs/InGaPN quantum wells grown by MOVPE", (2010) *Physica E: Low-dimensional Systems and Nanostructure*, **42**, 1176–1179.

[2] **D. Kaewket**, S. Sanorpim, S. Tungasmita, R. Katayama and K. Onabe, "Photoluminescence study of type-II InGaPN/GaAs quantum wells" (2010) *Journal of Nanoscience and Nanotechnology*, **10**, 7154-7157.

[3] **D. Kaewket**, S. Sanorpim, S. Tungasmita, R. Katayama and K. Onabe, "MOVPE growth of high optical quality InGaPN layers on GaAs (001) substrates", (2010) *Physica Status Solidi C*, **7**, 2079-2081.

2. Manuscript for submission

[1] **D. Kaewket**, S. Sanorpim, S. Tungasmita, R. Katayama and K. Onabe, "Photoluminescence and Raman Scattering of InGaPN on GaAs"

3. Presentations in international conferences

[1] **D. Kaewket**, S. Sanorpim, S. Tungasmita, R. Katayama and K. Onabe, "Band alignment of lattice-matched InGaPN/GaAs and GaAs/InGaPN quantum wells grown by MOVPE" *International Conference on Electronic Properties of Two-Dimensional Systems and Modulated Semiconductor Structures (EP2DS-18/MSS-14)*, Kobe, Japan, July 19-24, 2009.

[2] **D. Kaewket**, S. Sanorpim, S. Tungasmita, R. Katayama and K. Onabe, "Photoluminescence study of type-II InGaPN/GaAs quantum wells" *International Conference on Nanoscience & Technology, China 2009 (ChinaNANO 2009)*, Beijing, China, September 1-3, 2009.

[3] **D. Kaewket**, S. Sanorpim, S. Tungasmita, R. Katayama and K. Onabe, "MOVPE growth of high optical quality InGaPN layers on GaAs (001) substrates" *8th International Conference on Nitride Semiconductors (ICNS-8)*, Jeju, Korea, October 18-23, 2009.

[4] **D. Kaewket**, S. Sanorpim, S. Tungasmita, R. Katayama and K. Onabe, "Photoluminescence and band lineup of InGaPN/GaAs quantum wells" *NanoThailand 2010*, Bangkok, Thailand, November 18-20, 2010.

4. Presentations in domestic conferences

[1] **D. Kaewket**, S. Sanorpim, S. Tungasmita, R. Katayama and K. Onabe, "Promising of dilute III-(III)-V-nitride semiconductors for solar cell applications" *Siam Physics congress 2009,* Phetburi, Thailand, March 19-21, 2009.

[2] **D. Kaewket**, S. Sanorpim, S. Tungasmita, R. Katayama and K. Onabe, "Photoluminescence and band alignment of InGaPN/GaAs bulk and quantum wells" *36th Congress on Science and Technology of Thailand (STT 36)*, Bangkok, Thailand, October 26-28, 2010.

[3] **D. Kaewket**, S. Sanorpim, S. Tungasmita, R. Katayama and K. Onabe, "Photoluminescence and band lineup of InGaPN/GaAs quantum wells" *The Science Forum 2011*, Faculty of Science, Chulalongkorn University, Thailand, March 10-11, 2011.

[4] **D. Kaewket**, S. Sanorpim, S. Tungasmita, S. Kuboya and K. Onabe, "Photoluminescence and raman scattering of InGaPN/GaAs grown by MOVPE" *Siam Physics congress 2011*, Pattaya, Thailand, March 23-26, 2011.

[5] **D. Kaewket**, S. Sanorpim, S. Tungasmita, R. Katayama and K. Onabe, “Band alignment of InGaPN/GaAs quantum wells grown by MOVPE” *RGJ-Ph.D. Congress XII*, Pattaya, Thailand, April 1-3, 2011.

VITAE

Miss Dares Kaewket was born on October 13, 1981 in Phitsanulok, Thailand. She received her Bachelor degree of Science in Physics from Chulalongkorn University in 2003. She received her Master degree of Science in Physics from Chulalongkorn University in 2006. And she continued her Doctoral degree of Science in Physics at Chulalongkorn University in 2007.

During Doctoral studying, she spent time about ten months in Japan to learn about metalorganic vapor phase epitaxy (MOVPE) growth technique and use equipments for measuring high resolution X-ray diffraction, photoluminescence and photoreflectance at Professor Dr. Kentaro Onabe's laboratory, Department of Advanced Materials, The University of Tokyo. Moreover, she spent time about three months in Sweden to learn about micro-photoluminescence and time-resolve photoluminescence at Professor Dr. Per Olof Holtz's laboratory, Department of Physics (IFM), Linköpings University.